

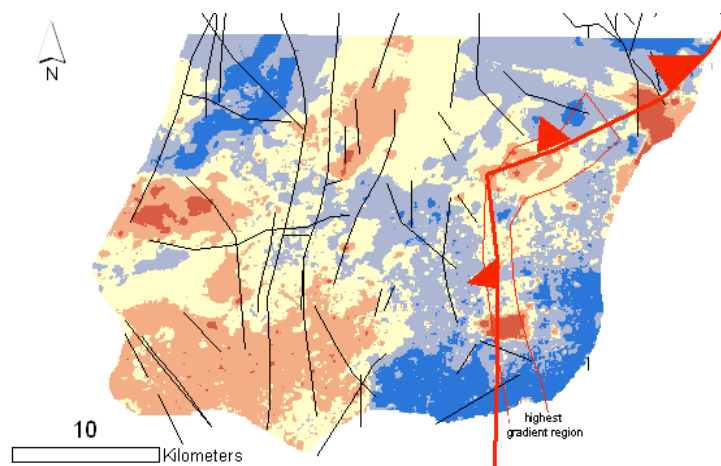
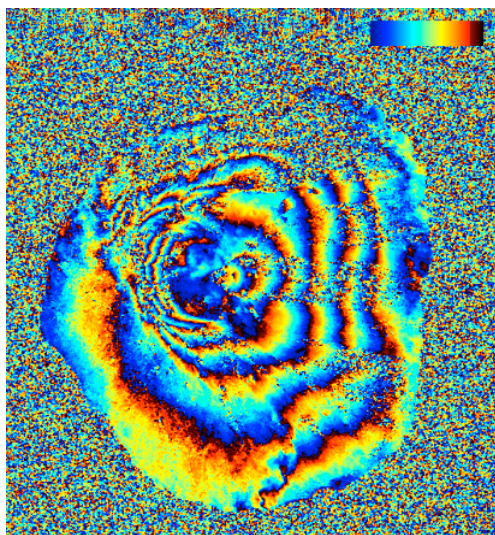


SEMINÁRIO ICIST

14 de fevereiro de 2008

Aplicações de Interferometria de Radar na Área dos Riscos Geológicos

Sandra I. N. Heleno

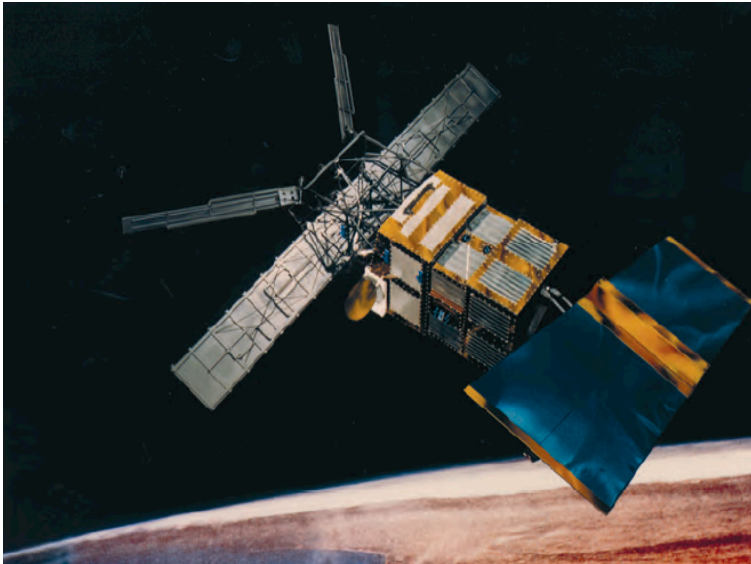


Synthetic Aperture Radar (SAR)

- Microwave imaging system (cloud penetration).
- Active system (day and night operational capabilities)
- Single wavelength (5.6 cm for ERS and ENVISAT)
- Coherent radiation, allows interferometry

ERS-2

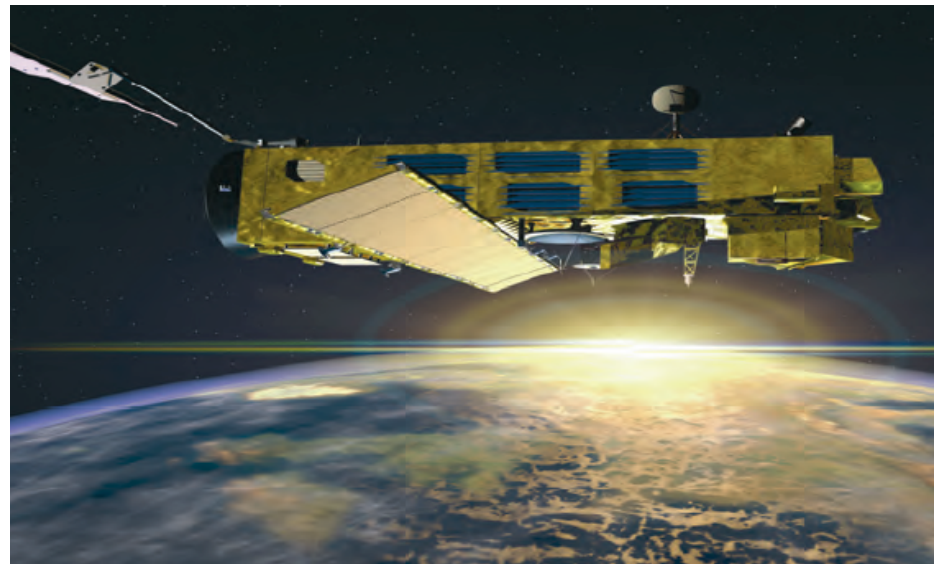
(launched in 1995 following ERS-1 in 1991)



Source: ESA, 2007

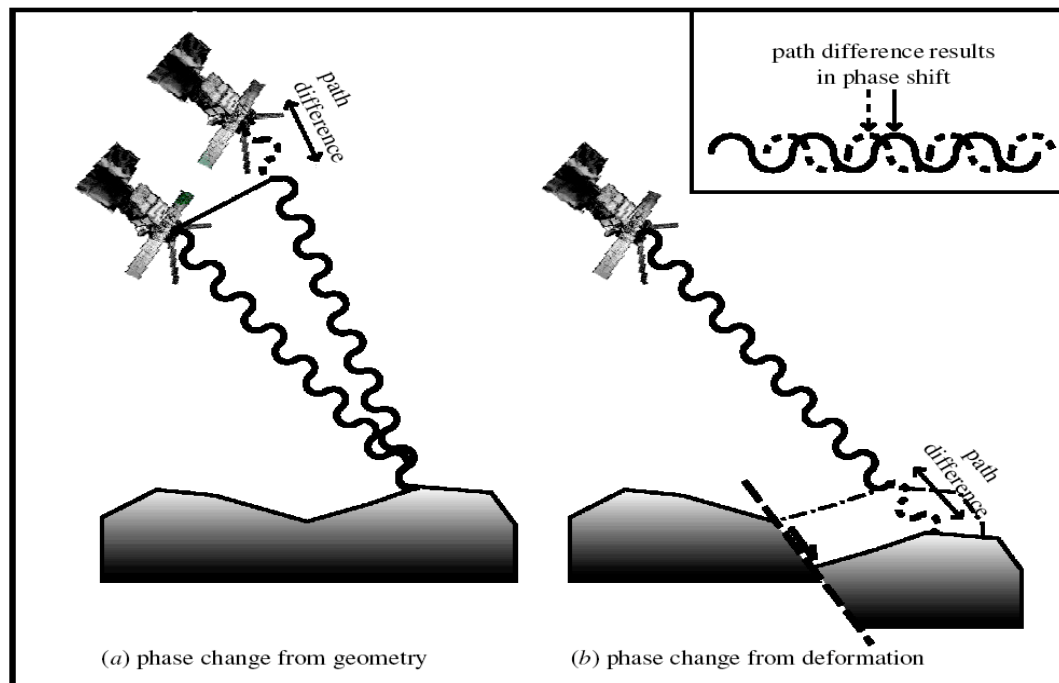
ENVISAT

(launched in 2002)



Source: ESA, 2007

- Scatterers at different distances from the radar introduce different two-way travel delays.
- Due to the almost purely sinusoidal nature of the transmitted signal, the difference in delay can be measured from the phase shift it produces.

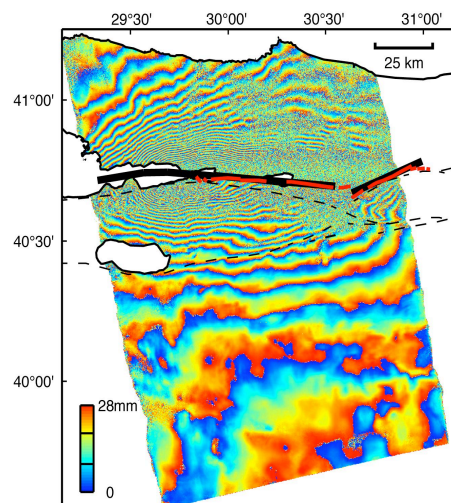


Source: Wright, 2002

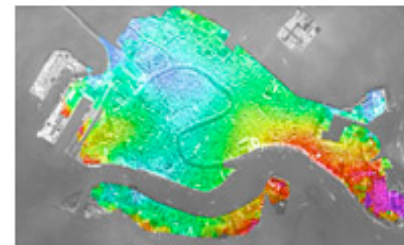
- The interferogram is generated from a pair of complex SAR images: for each pixel (25mx25m), its phase is the phase difference between the images.

Processing:

The two images must first be co-registered, using a correlation procedure to find the offset and difference in geometry between the two amplitude images. One SAR image is then re-sampled to match the geometry of the other. The interferogram is then formed, and the interferometric phase due to the orbital geometry and the reference ellipsoid is removed, as well as the phase due to topography (using a DEM of the area).



Izmit, 1999 (source: ESA)



SAR Interferometry shows edges of Venice in motion

Source: ESA

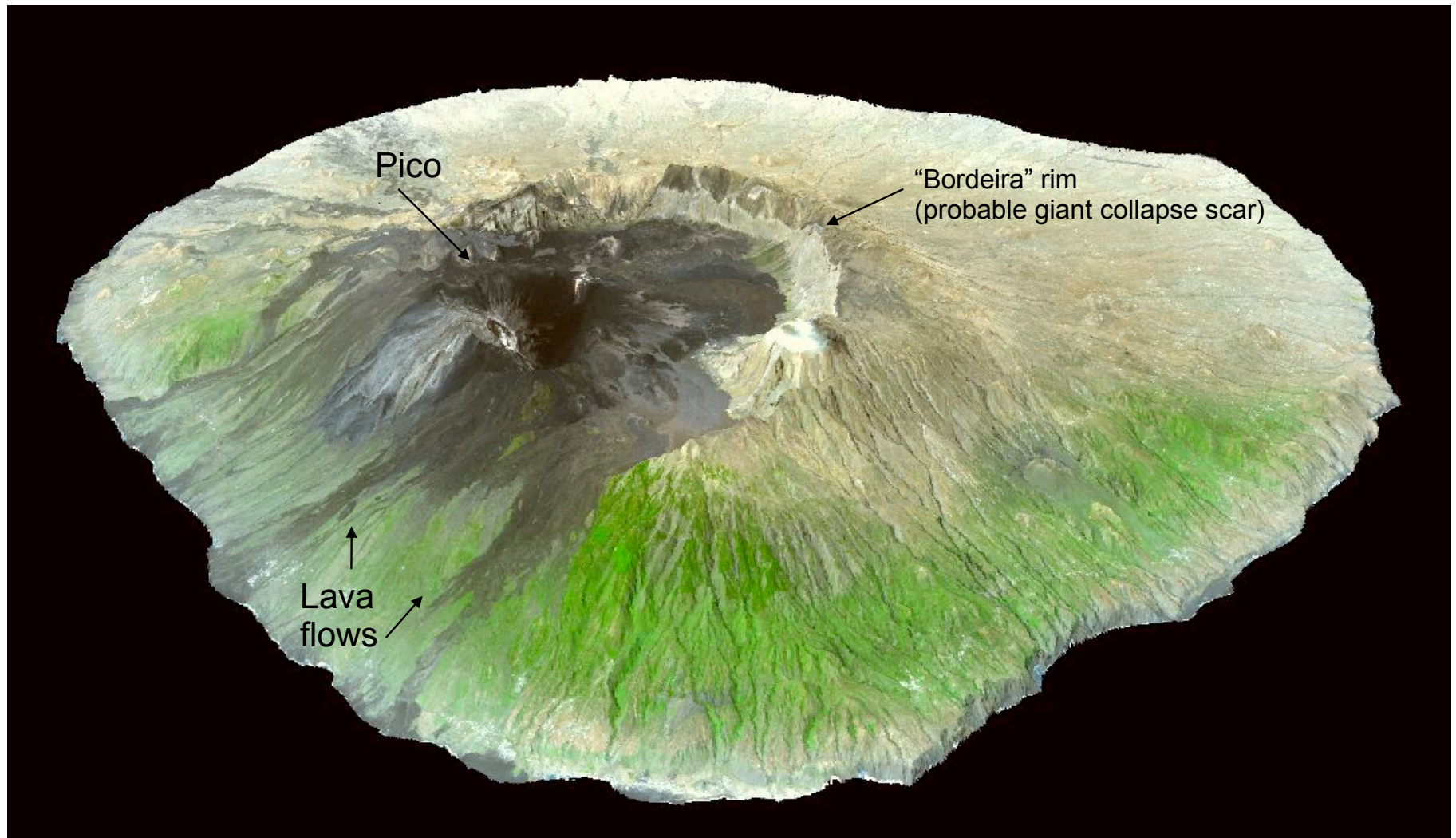


Fogo Volcano,
Cape Verde Islands

Source: NASA Aqua

ICIST Feb 2008

View from the NE



Source: NASA/GSFC/METI/ERSDAC/JAROS,
and U.S./Japan ASTER Science Team

ICIST Fev 2008

ESA cat-1 SAMAAV – SAR Monitoring of Active African Volcanoes

SAMAAV – Fogo InSAR processing

1993 to 2007 period --> over 150 interferograms

10 ERS1 SLC images (track 460, pass A) from Feb 1993 to Nov 1995

14 ERS2 SLC images (track 460, pass A) from Nov 1995 to Nov 2002

75 two-pass deformation interferograms computed with **Bperp < 500m**

software: **DORIS** InSAR processor (using **DEOS precise orbits** and **SRTM90 DEM**)

7 ERS2 SLC images (track 252, pass D) from Jul 1997 to Oct 2002

16 two-pass deformation interferograms computed with **Bperp < 500m**

software: **DORIS** InSAR processor (using **DEOS precise orbits** and **SRTM90 DEM**)

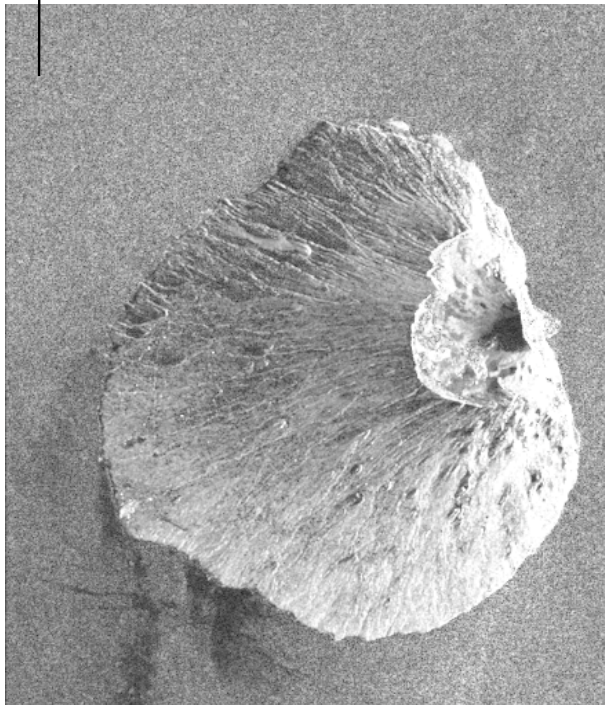
24 ENVISAT SLC images (track 460 I2, pass A) from July 2004 to September 2007

71 two-pass deformation interferograms computed with **Bperp < 500m**

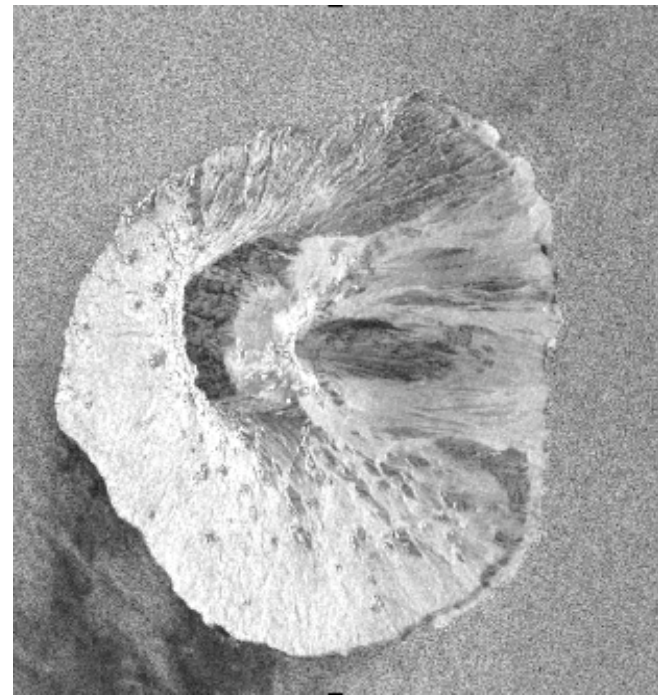
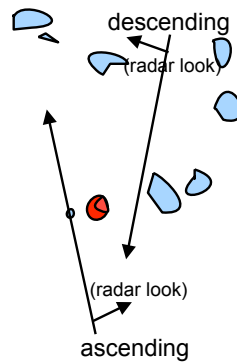
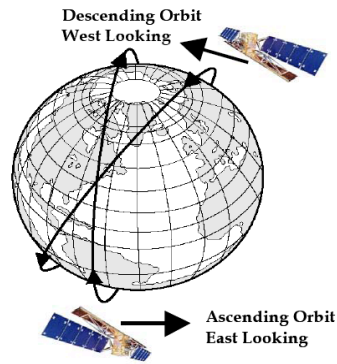
software: **DORIS** InSAR processor (using **DEOS precise orbits** and **SRTM90 DEM**)

Due to Fogo's steep slopes (up to 28°), the East flank can only be observed from ascending (nigh time) orbits while the West flank is better observed from descending (day time) orbits

N
↑



Descending (track 252)

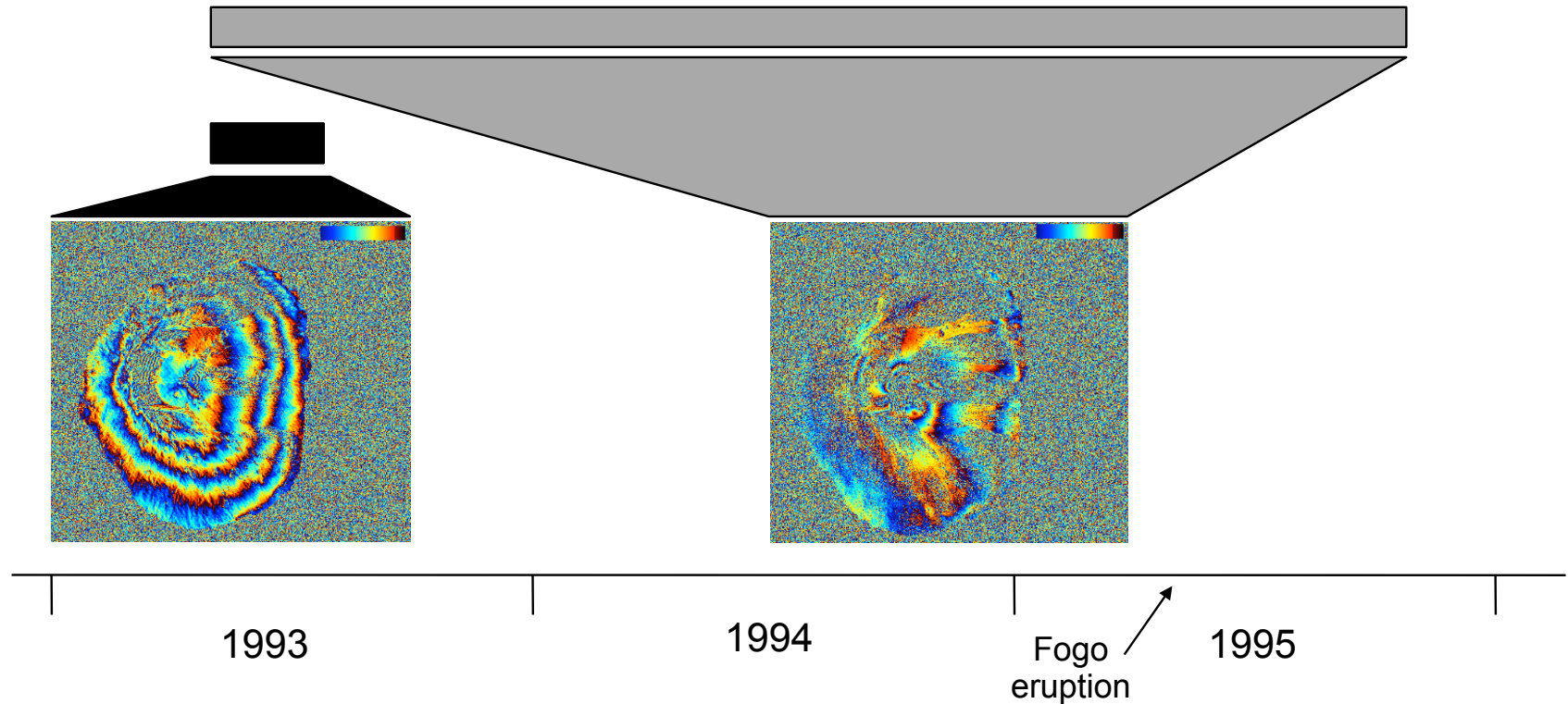


Ascending (track 460)

ERS before and encompassing Fogo's 1995 eruption

19 May 93 (ers1, 9623) – 28 July 93 (ers1, 10625): apparent inflation of the island
4 fringes ~ 11 cm

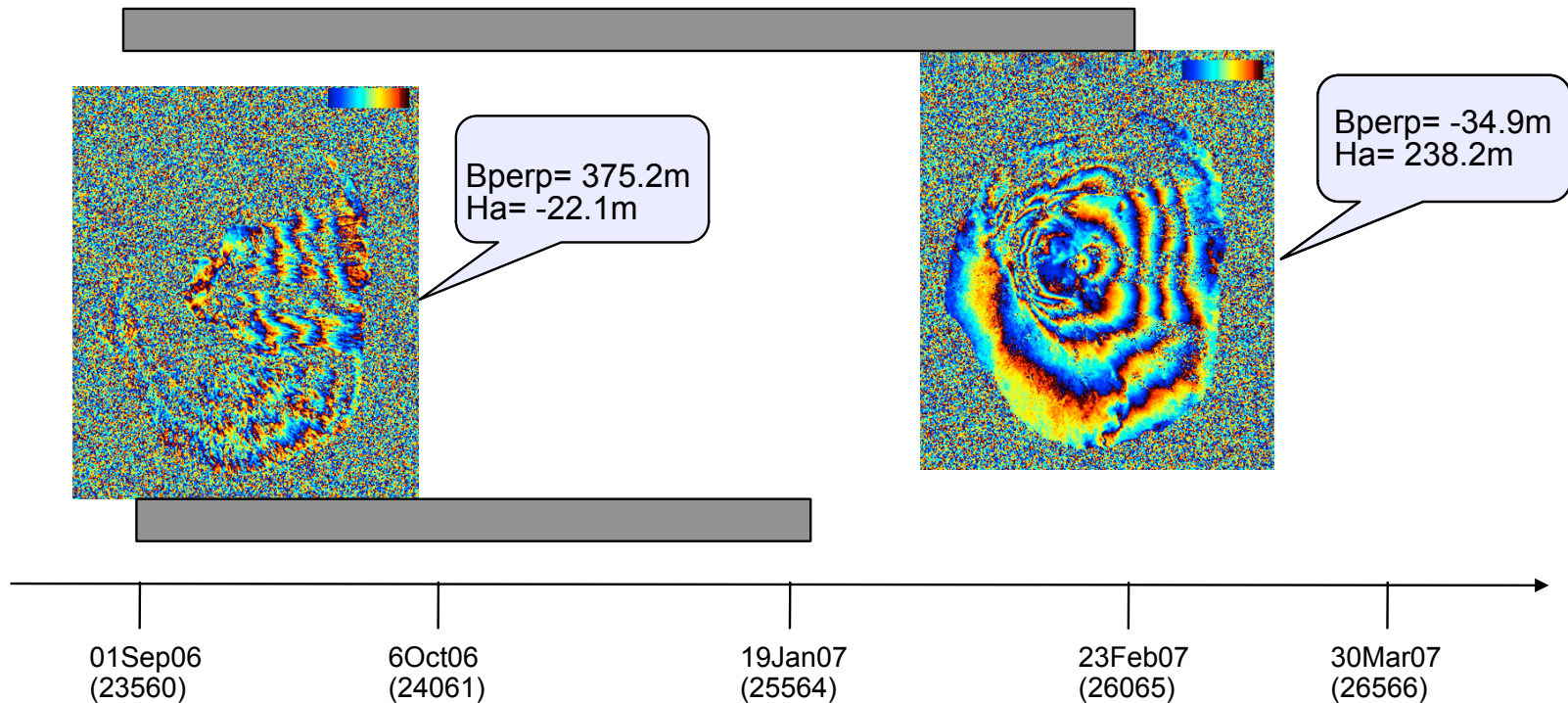
19 May 93 (ers1, 9623) – 3 November 95 (ers1, 22492): smaller scale deformation
interpreted by Amelung et al (2002) as related with 1995's eruption feeder dyke



Strong correlation between fringes and topography

Errors in DEM can be ruled out as the cause -- from comparison of altitudes of ambiguity between interferograms

One example: both envisat interferograms show approximately 5 fringes on collapse scar fill, but the altitudes of ambiguity are radically different (-22.1m and 238.2 m)



Source: wikipédia

Interferometric phase contributions:

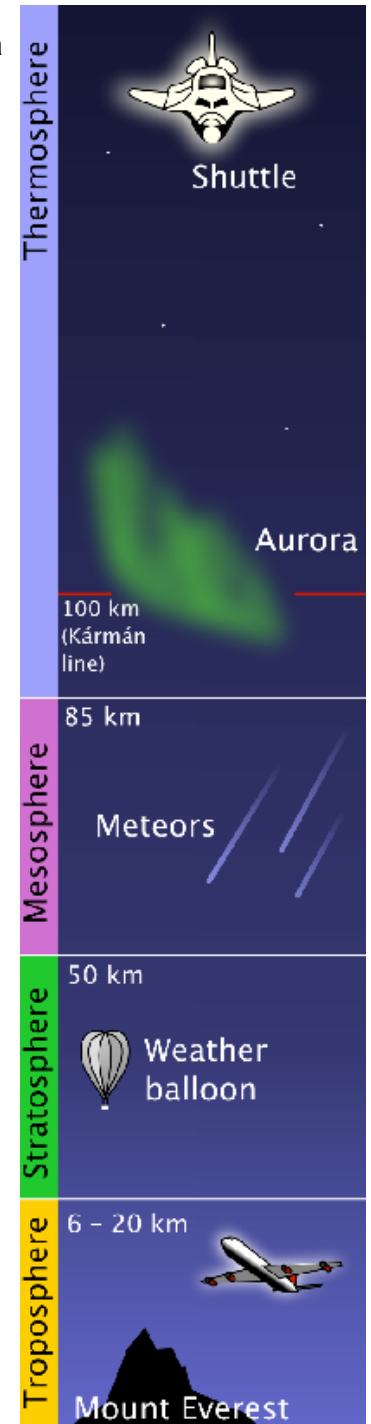
$$\phi = \phi_{\text{topo}} + \phi_{\text{defo}} + \phi_{\text{iono}} + \phi_{\text{na}} + \phi_{\text{orbit}} + \phi_{\text{ref}} + \phi_{\text{noise}}$$

iono=ionosphere
na=neutral atmosphere

Atmospheric phase contributions:

Ionospheric effects in InSAR typically result in phase trends with long wavelengths

The dominant atmospheric contribution to phase variability is the spatial and temporal fluctuation in water vapor content in the troposphere



Source: wikipédia

Interferometric phase contributions:

$$\phi = \phi_{\text{topo}} + \phi_{\text{defo}} + \phi_{\text{iono}} + \phi_{\text{na}} + \phi_{\text{orbit}} + \phi_{\text{ref}} + \phi_{\text{noise}}$$

iono=ionosphere
na=neutral atmosphere

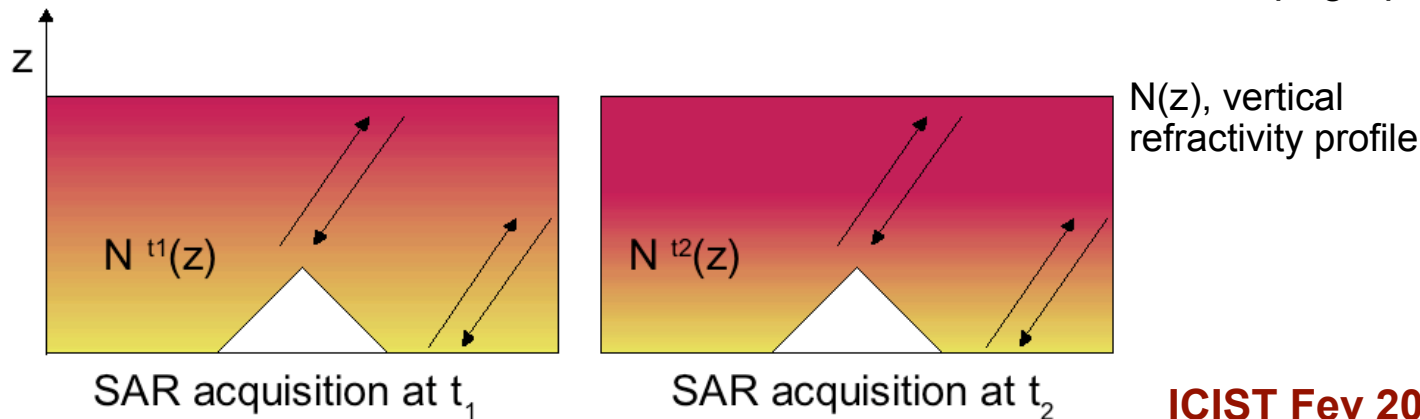
Atmospheric phase contributions:

Ionospheric effects in InSAR typically result in phase trends with long wavelengths

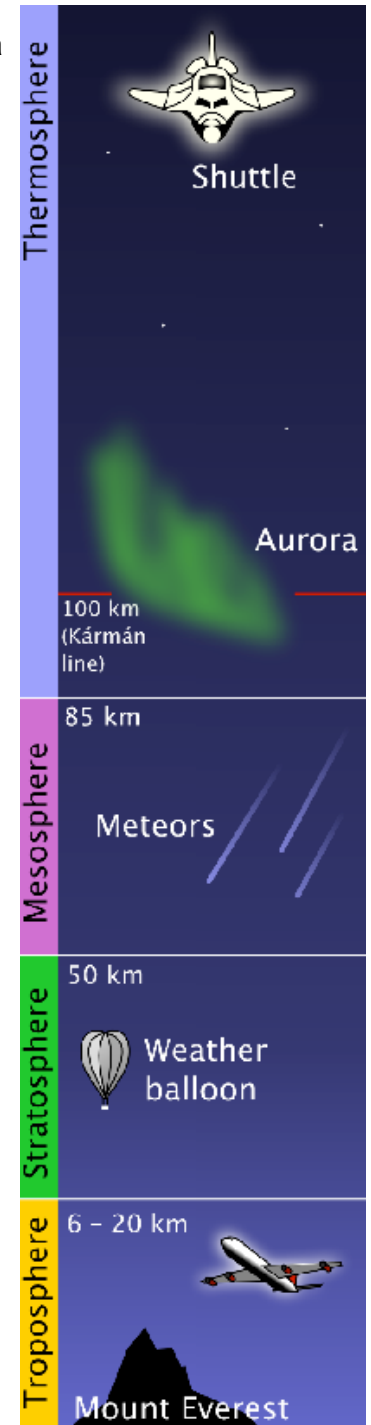
The dominant atmospheric contribution to phase variability is the spatial and temporal fluctuation in water vapor content in the troposphere

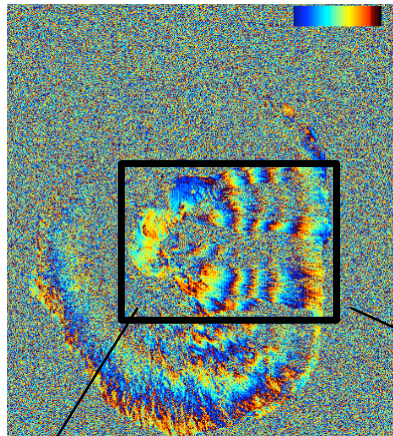
Atmospheric stratification:

results in tropospheric phase delay spatially correlated with topography



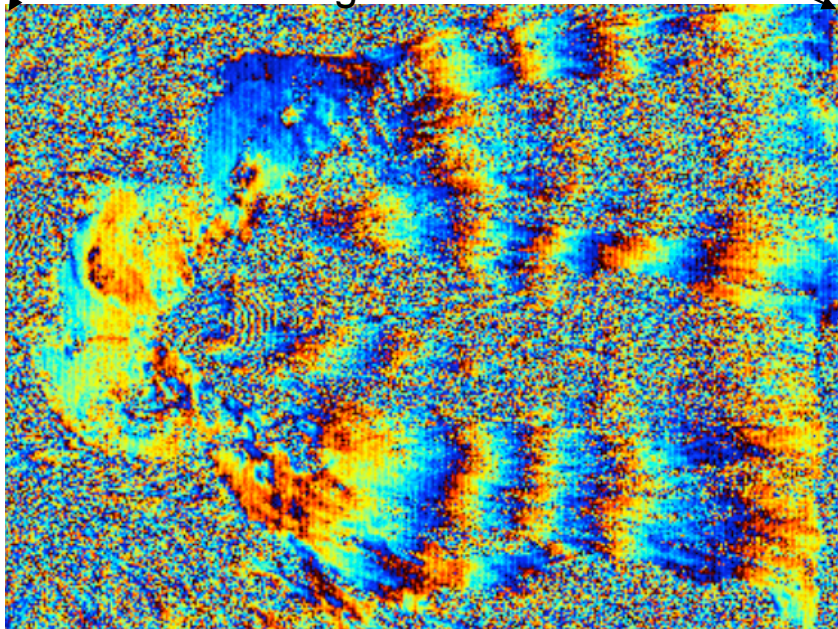
ICIST Fev 2008





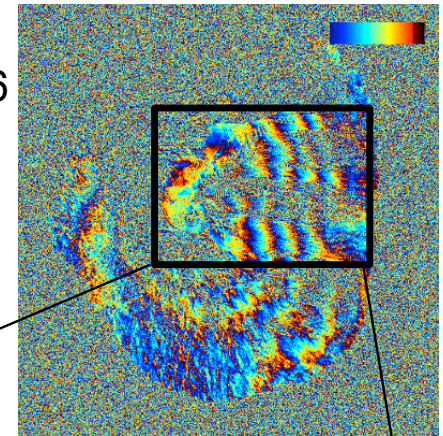
Master : 12 August 05
Slave: 10 March 06

4.5 fringes ~12.5 cm

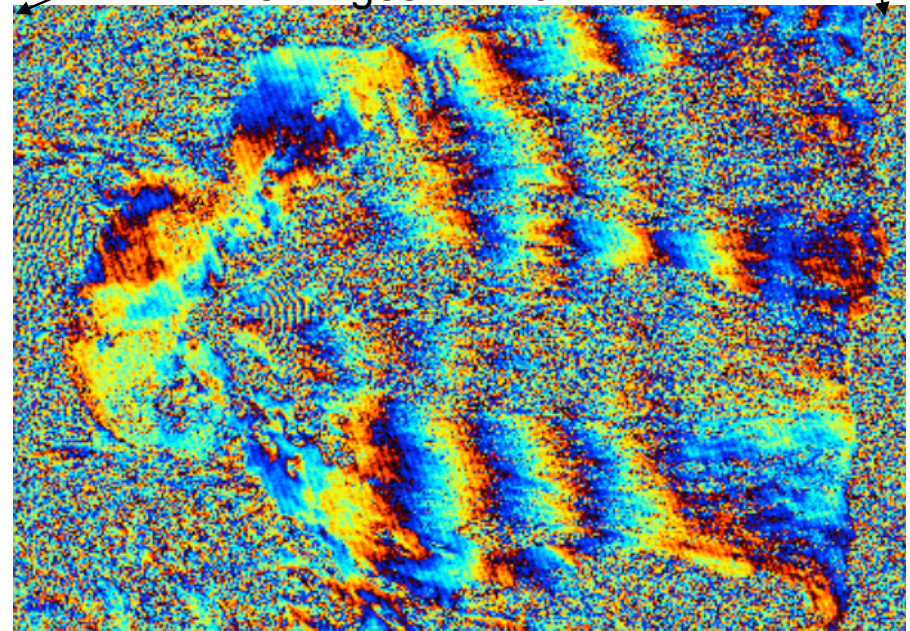


 Red-Yellow-blue (RYB) – from the volcanic centre to the coast

Master : 19 May 06
Slave: 1 September 06




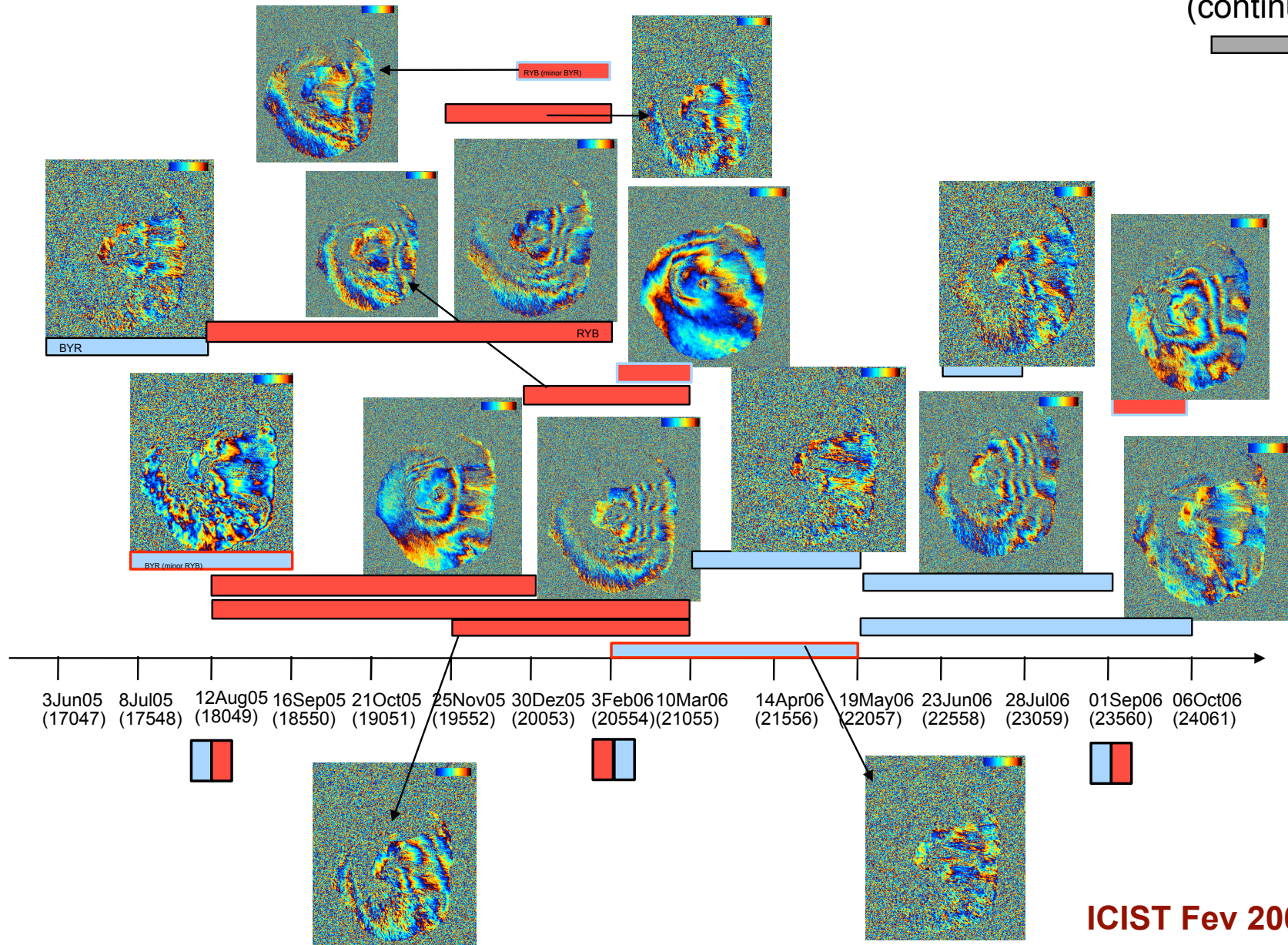
5 fringes ~ 14 cm



 Blue-Yellow-Red (BYR) – from the volcanic centre to the coast

ENVISAT ascending, track 460 I2 – from June 2005 through August 2007

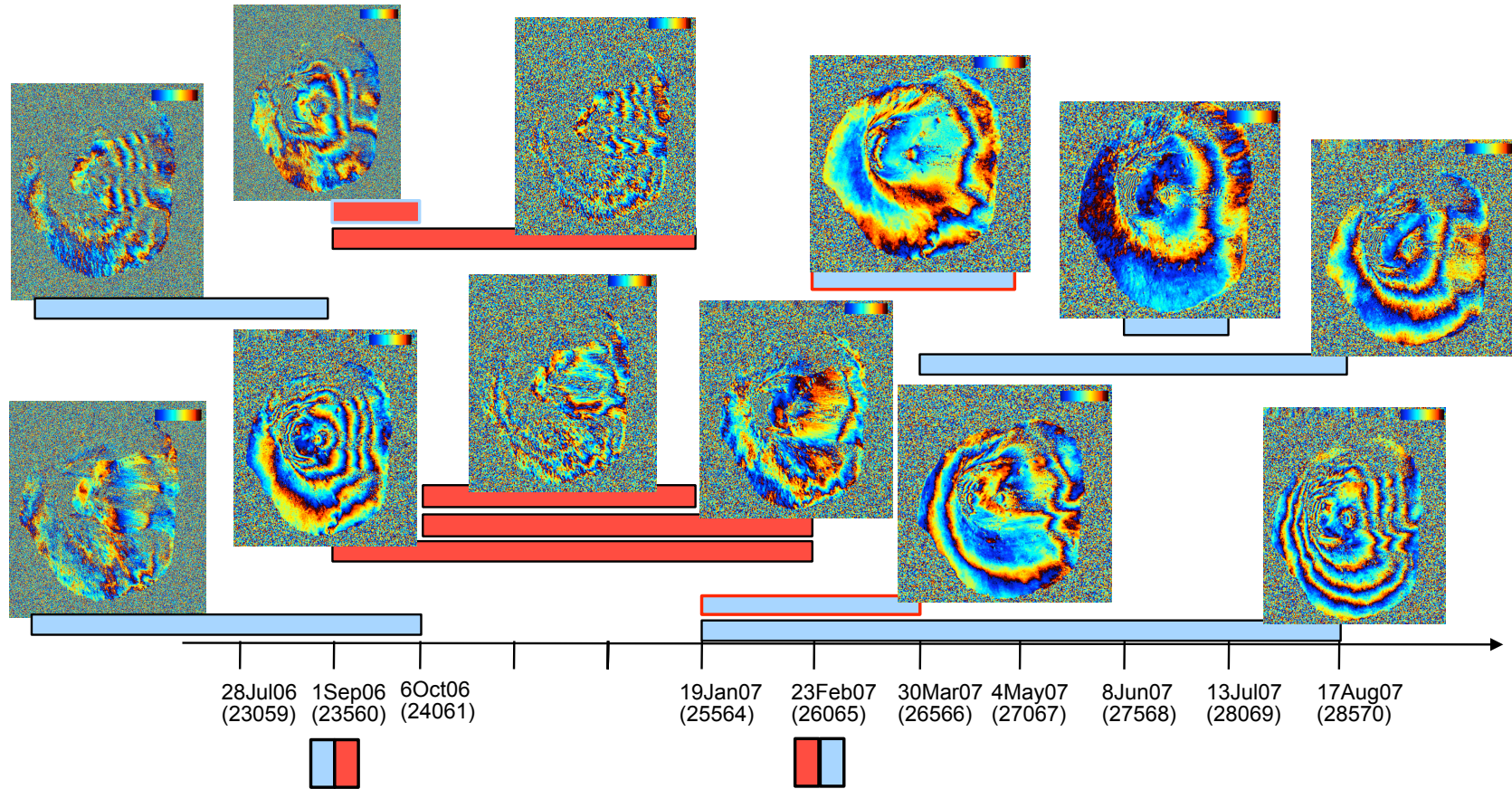
(continues...)




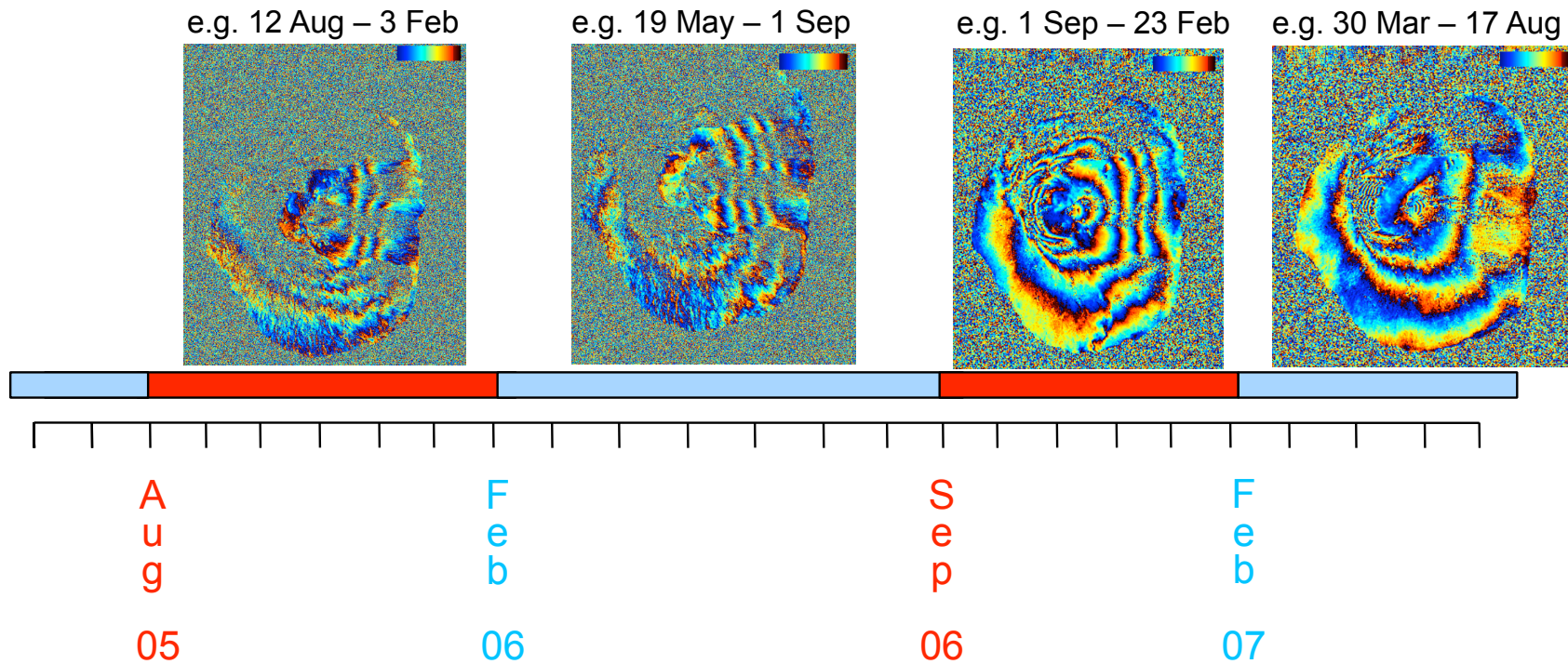
ICIST Feb 2008

ENVISAT ascending, track 460 I2 – from June 2005 through August 2007

(continuation)



ENVISAT – 2 YEARS – from June 2005 through August 2007



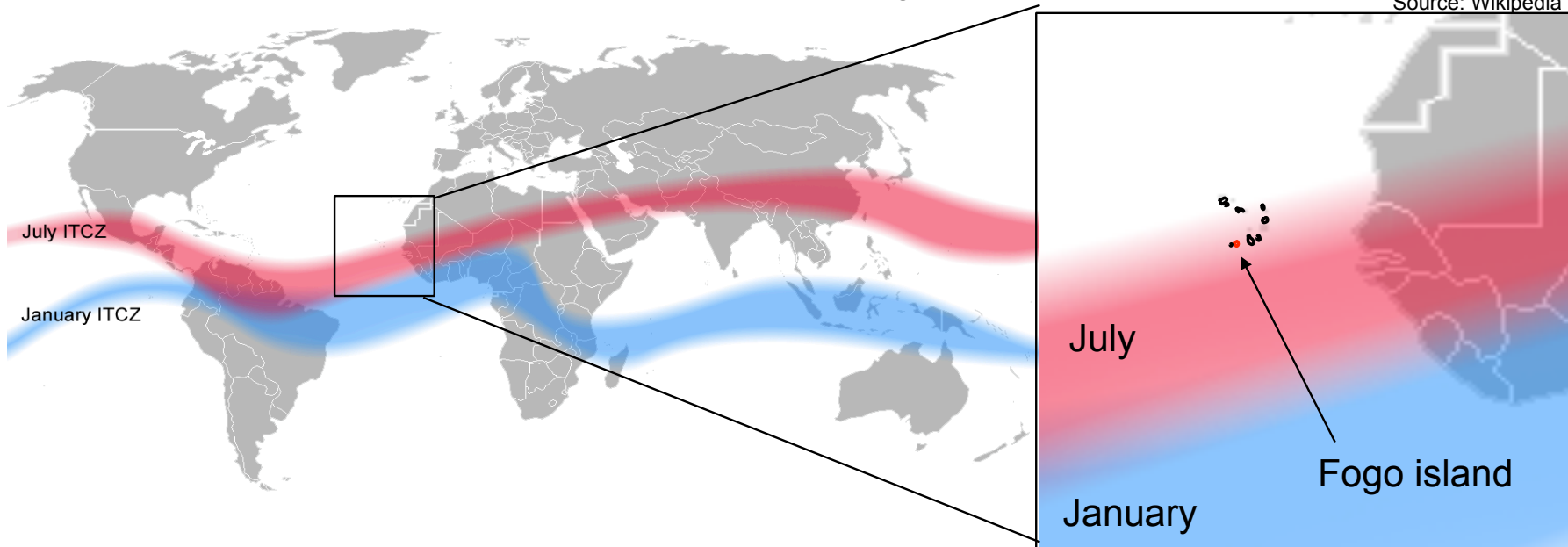
Can seasonal fluctuations of water vapour content in the Cape Verde region's troposphere explain this cyclic behaviour?

Can seasonal fluctuations of water vapour content in the Cape Verde region's troposphere explain this cyclic behaviour?

Cape Verde's wet season ("asaguas"): August, September and October

North-South oscillation of the Inter-tropical Convergence Zone (ITCZ)

Source: Wikipédia

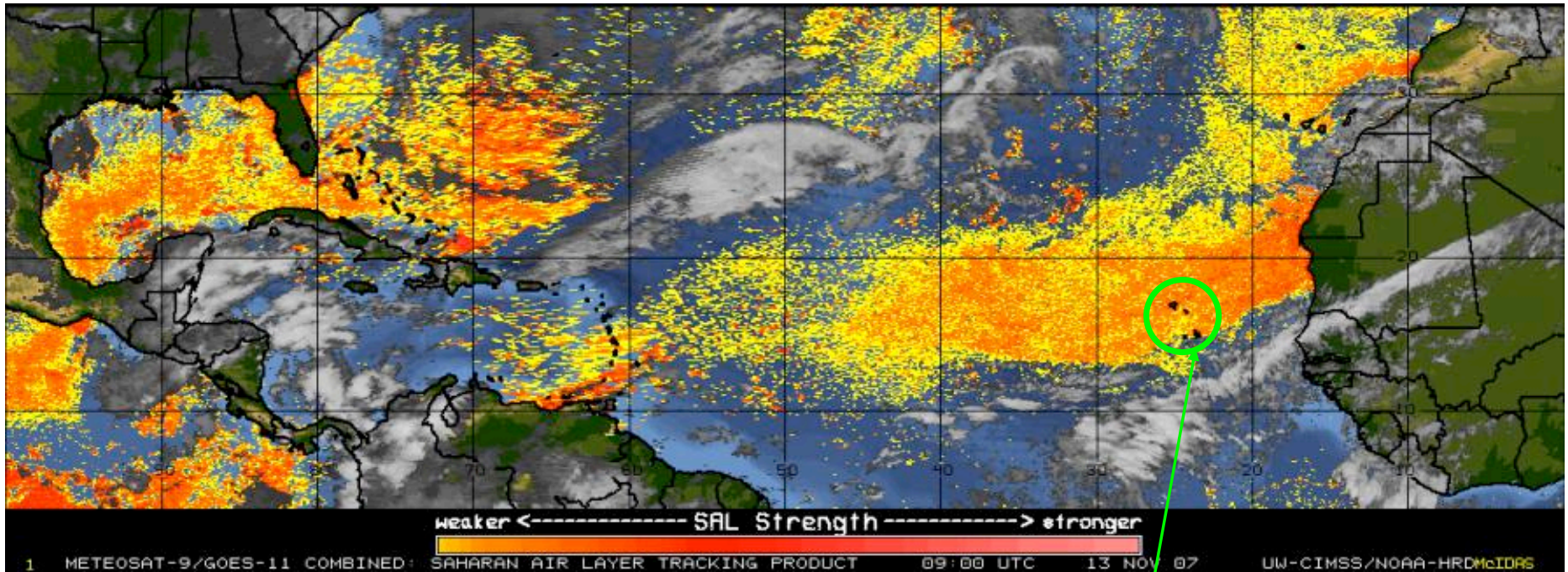


The **Inter-tropical Convergence Zone (ITCZ)** is a belt of low pressure surrounding Earth at the equator, formed by the vertical ascent of warm, **moist** air.

Can seasonal fluctuations of water vapour content in the Cape Verde region's troposphere explain this cyclic behaviour?

Cape Verde's dry fog season (“bruma seca”): October to April

Saharan Air Layer : warm, **dry** and dusty air layer (900m-5500m) transported from the Sahara



Cape Verde
Islands

ICIST Feb 2008

MODIS precipitable water vapor (PWV) product consists of column water-vapor amounts in centimeters

The data is collected by the Terra and Aqua NASA satellites, and freely distributed in the internet

During the daytime, a near-infrared algorithm is applied (PWVNIR), that is based on detecting the absorption by water vapor of the reflected solar radiation.

The PWVNIR (daytime) results are produced with 1-km spatial resolution over areas where there is a reflective surface in the near IR:

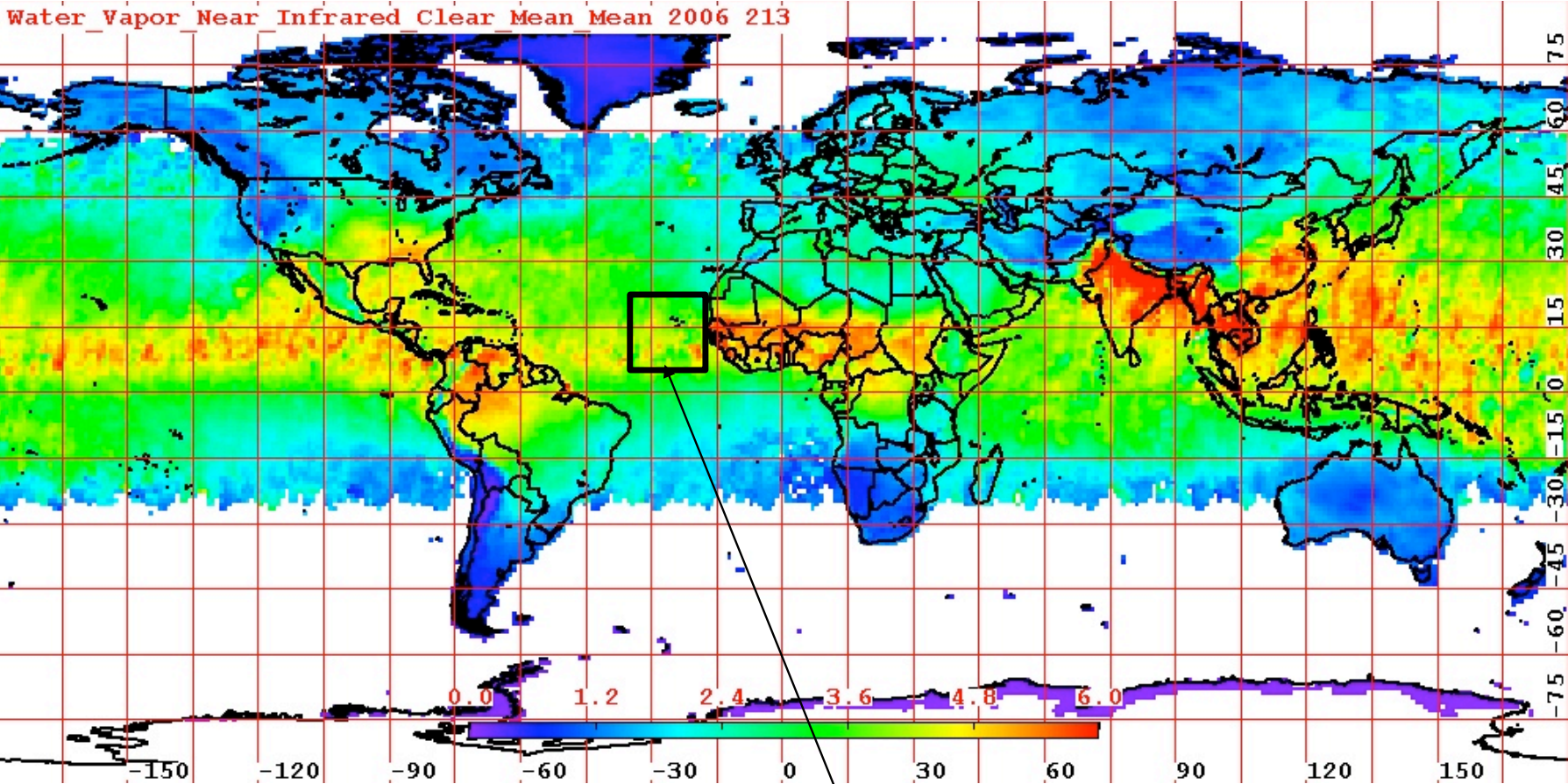
- 1) clear (cloud-free) land areas
- 2) above clouds
- 3) clear ocean areas with glint

An infrared algorithm (PWVIR) is also applied both day and night, by integrating the moisture profile through the atmospheric column.

The results depend in part on the initial guess for the temperature and moisture profiles used in the inversion. Over land, the technique works better over areas covered by green vegetation (Gao & Kaufman, 2003, JGR).

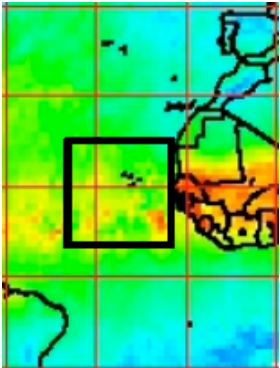
The PWVIR (both day and night time) results are produced with 5 x 5 1-km pixel resolution over clear (cloud free) land and ocean areas.

MODIS PWVNIR Monthly Average Product (August 2006)

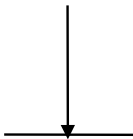


Cape Verde Islands

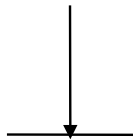
MODIS PWVNIR Monthly Average Product



DRYEST

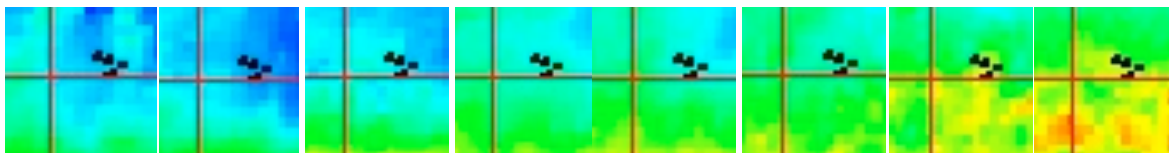


WETEST

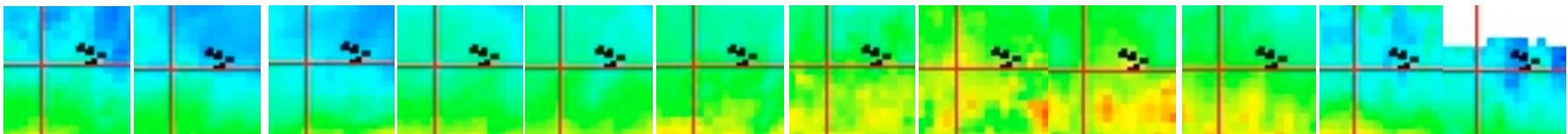


January February March April May June July August Septemb Octob Novemb Decemb

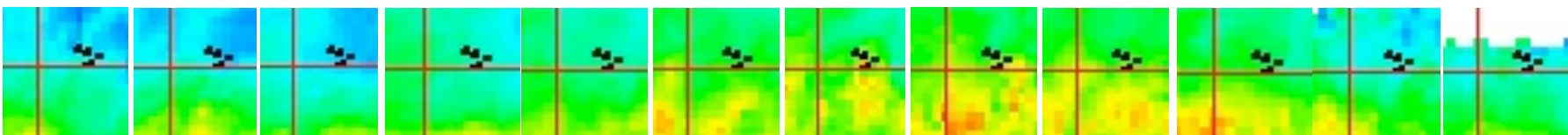
2007



2006



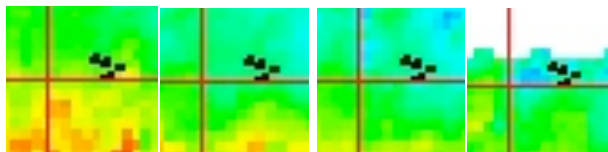
2005



2004

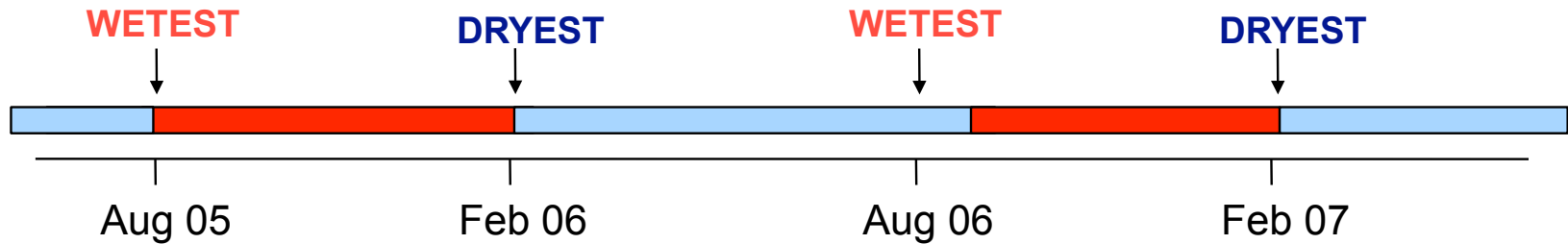
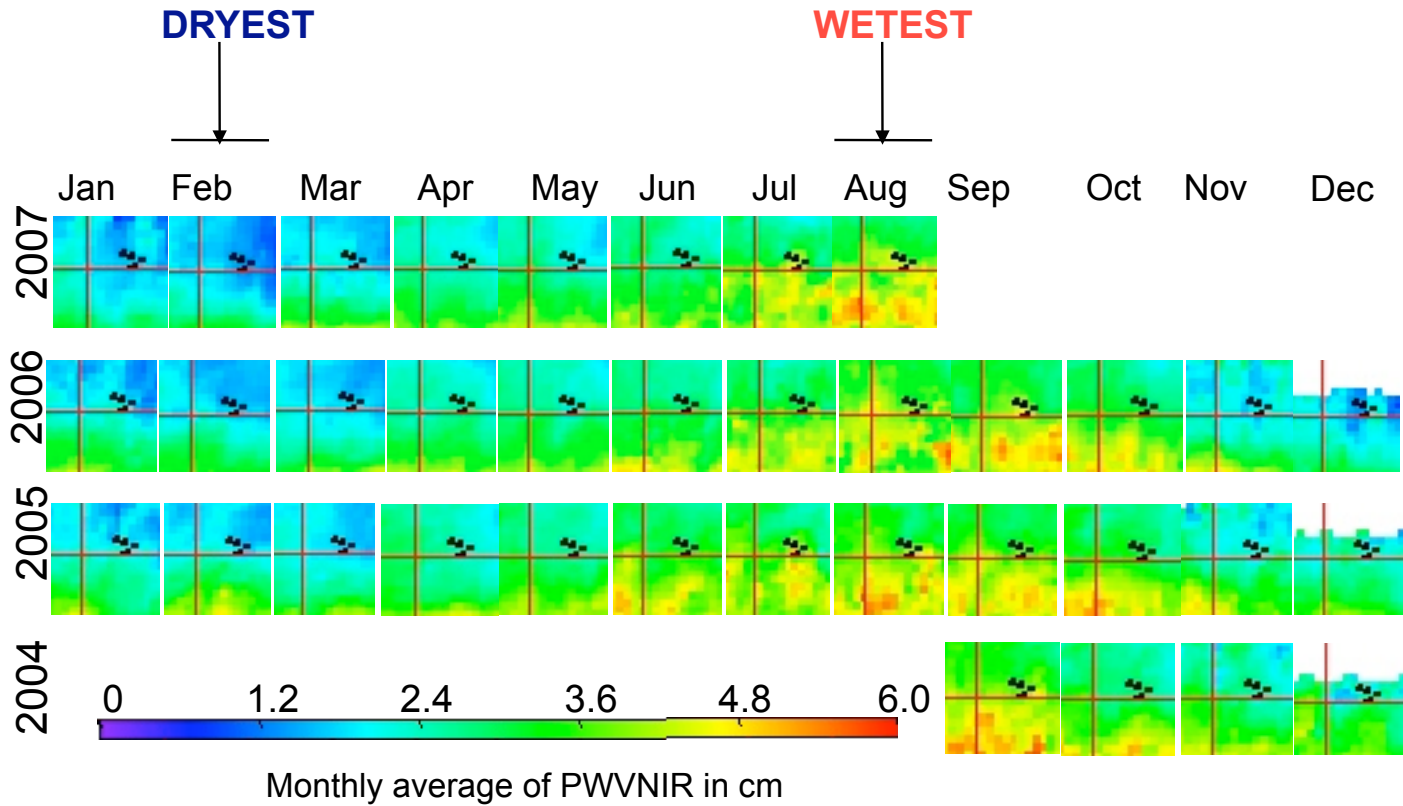
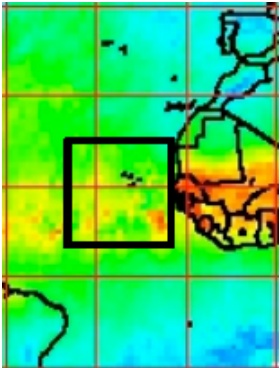


Monthly average of PWVNIR in cm



ICIST Feb 2008

MODIS PWVNIR Monthly Average Product



- . These results strongly indicate that most (if not all) of the phase variability observed - corresponding to apparent displacements of up to 14 cm either away or towards the satellite - is due to water vapor change in the troposphere!!**
- . Tropospheric water vapor variability is a know limitation of InSAR, specially in mountainous areas and in tropical climates. In Fogo the atmospheric effects are much stronger than what has been described at other volcanoes.**

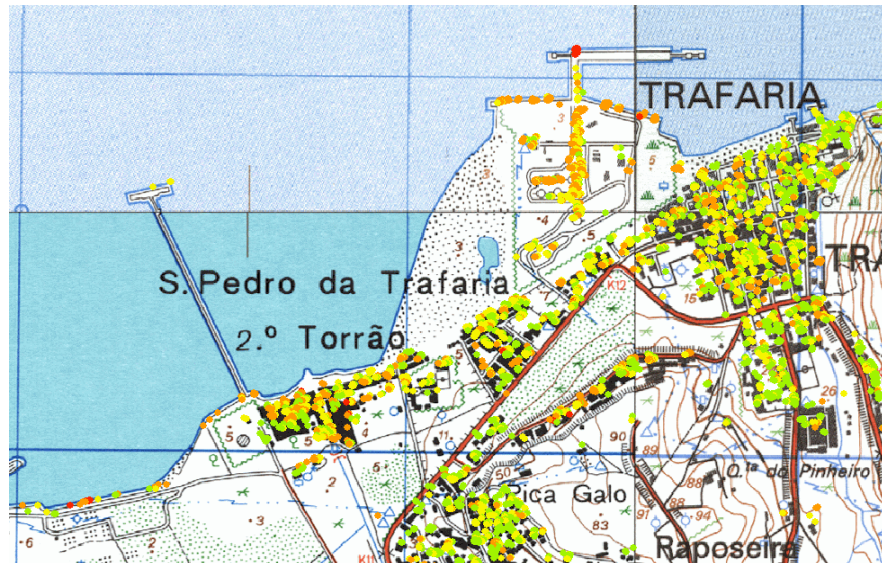
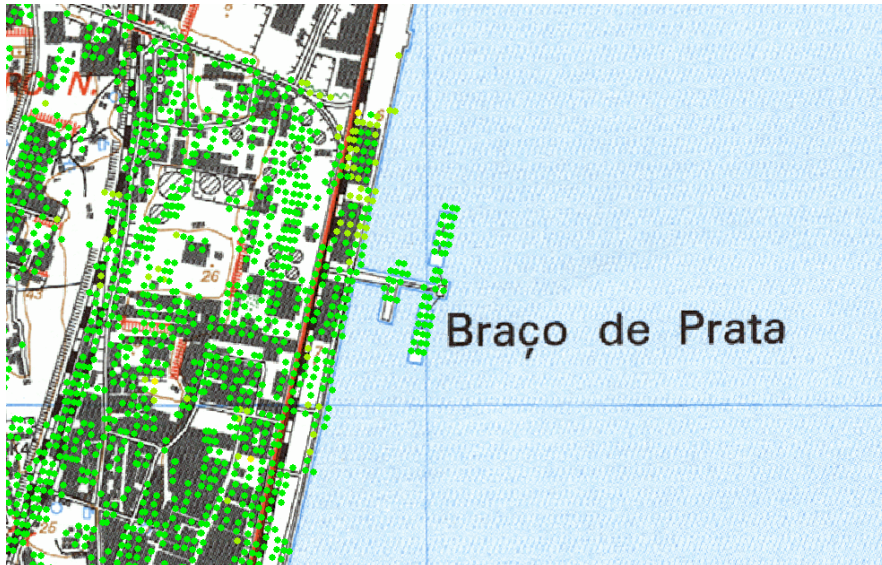
InSAR Limitations:

- Temporal and geometrical decorrelation
- Changes in tropospheric water vapor result in variable phase delay (effects are highest in tropical and sub-tropical regions)

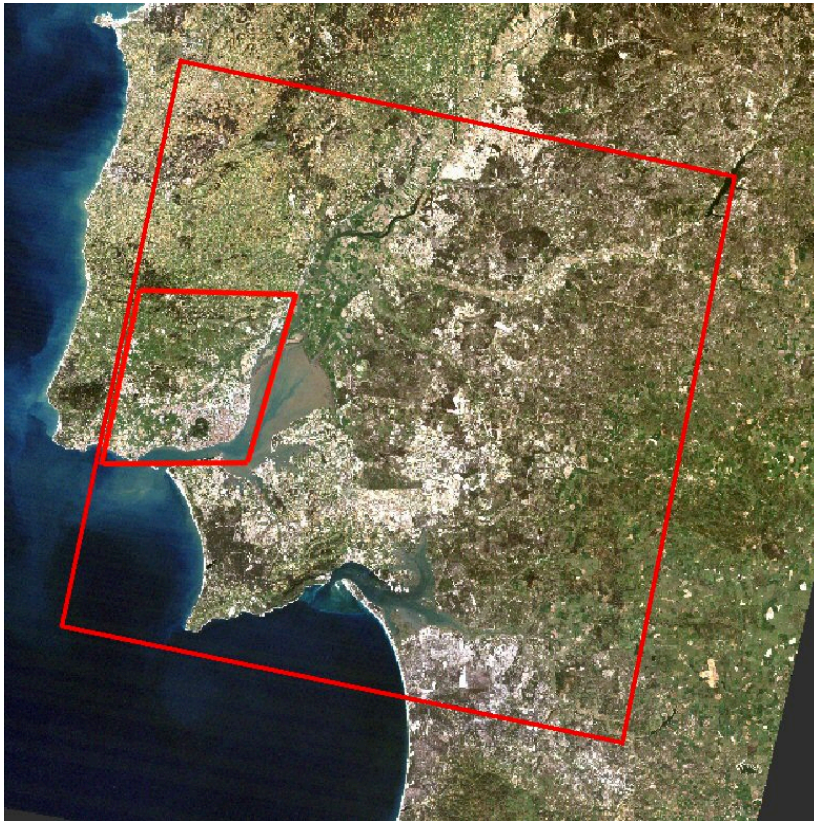
Permanent Scatterer InSAR (PSInSAR):

- Atmospheric effects are estimated and removed by combining data from long series of SAR images, averaging out the temporal fluctuations.
- Only radar scatterers that are minimally affected by temporal and geometrical correlation (permanent scatterers) are used.
- Surface deformation is usually assumed to be linear in time at each scatterer point.
- Man-made structures in urban settings constitute most of permanent scatterers.
- Vegetated areas have very few permanent scatterers, since vegetation undergoes motion and growth over the imaging period.

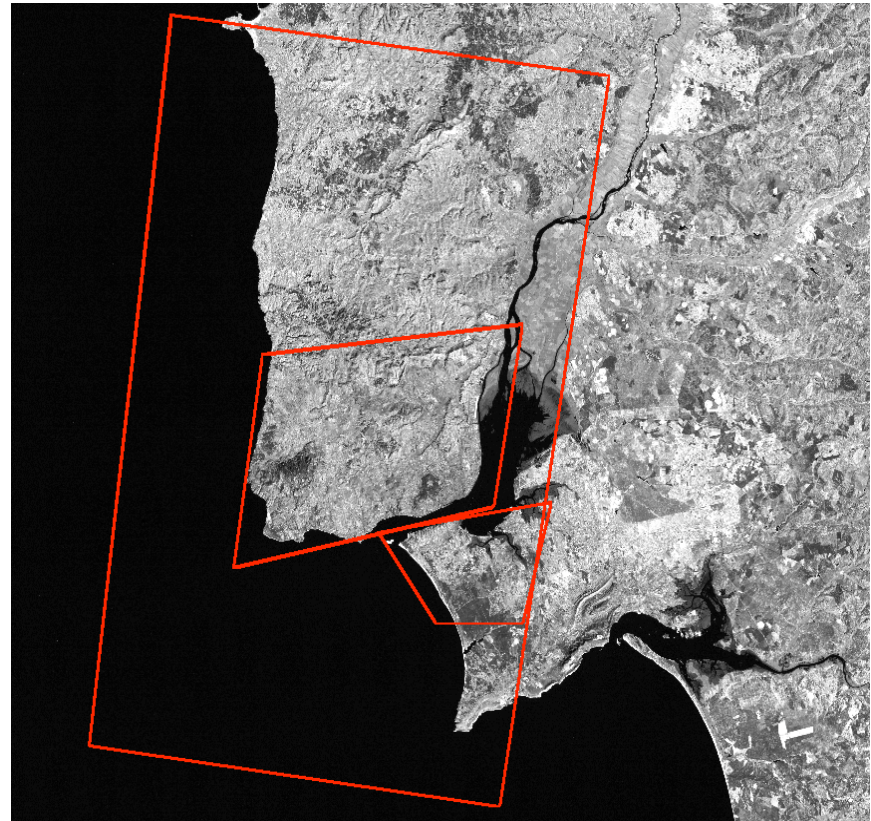
Examples of permanent scatterers in Lisbon:

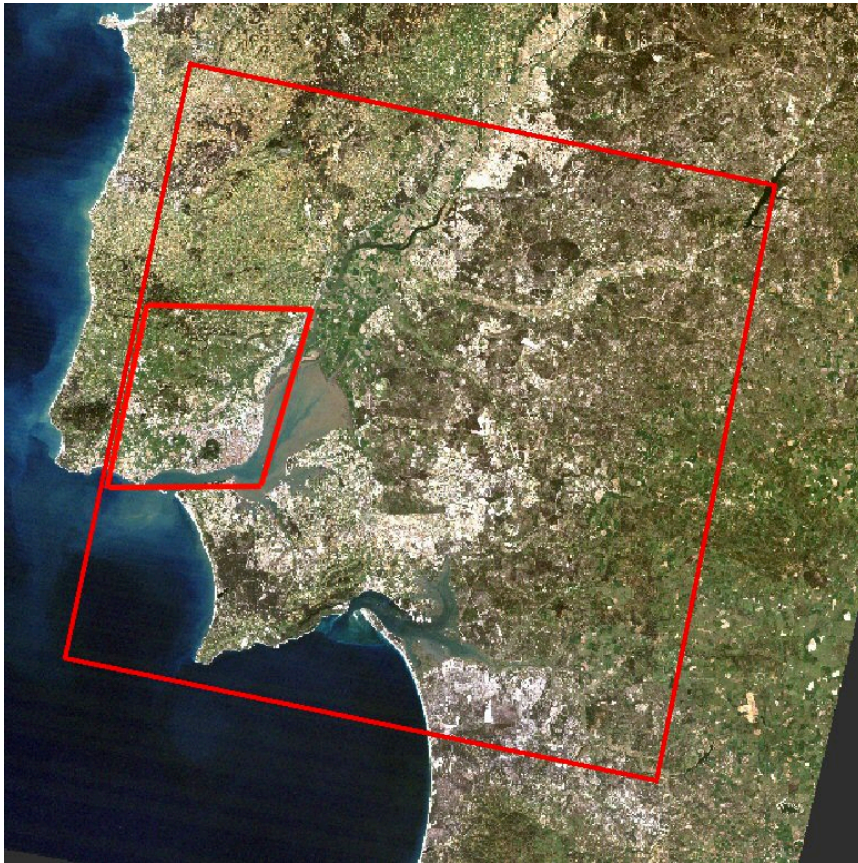


TRE, track 452, pass D
ERS1/2, 1992-2003



Altamira, track 223, pass D
ERS1/2 and Envisat, 1992-2006





TRE North Lisbon area

Process Date: 04 June 2004

Software used

TRE's PSInSAR processing chain

Analysis type: H1c

Number of scenes used: 55

Date range of analysis

2 June 1992 – 26 December 2003

Satellite data used: ERS -1/2

Master Scene Date: 07 March 1997

Georeference (X,Y) accuracy

± 4 m, ± 10 m

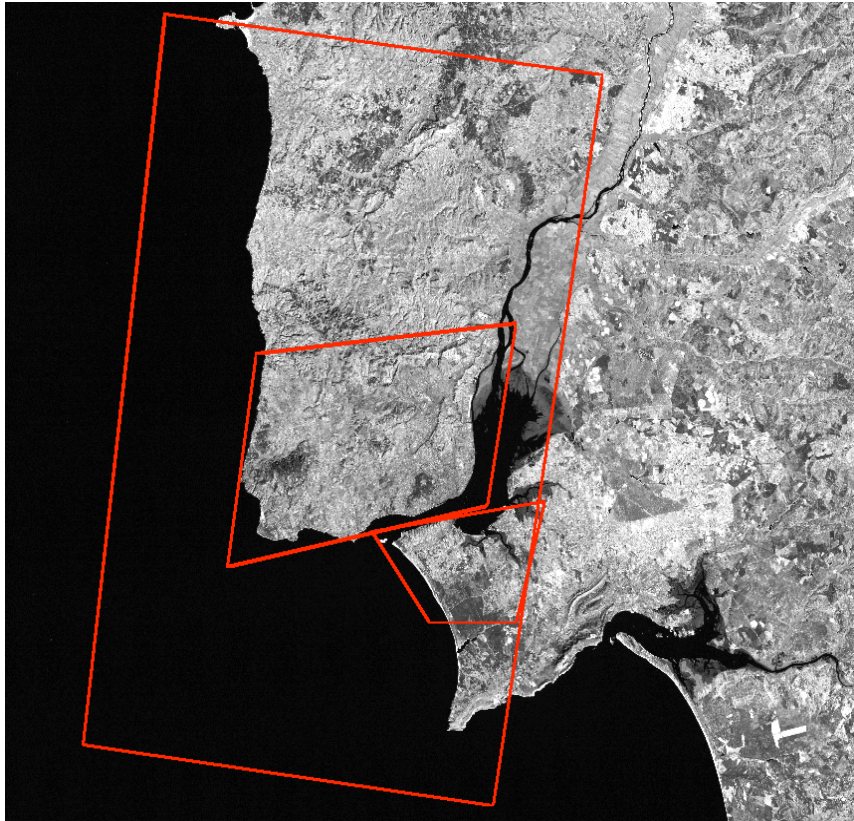
Projection system used: WGS84

Reference point location

Lat: 38.84882180

Lon: -9.17918142

Area of results: ~ 800 Km²



Altamira North Lisbon area

Process Date: 23 May 2007

Software used: SPN

Number of scenes used: 100

Date range of analysis: July 1992 to October 2006

Satellite data used: ERS -1/2 and Envisat

Georeference (X,Y) accuracy: 5 m

Reference point location: 487839.96E 4287647.38N

Altamira South Lisbon area

Process Date: 23 May 2007

Software used: SPN

Number of scenes used: 100

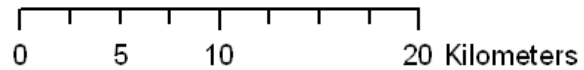
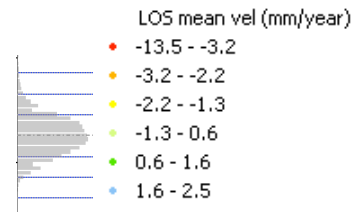
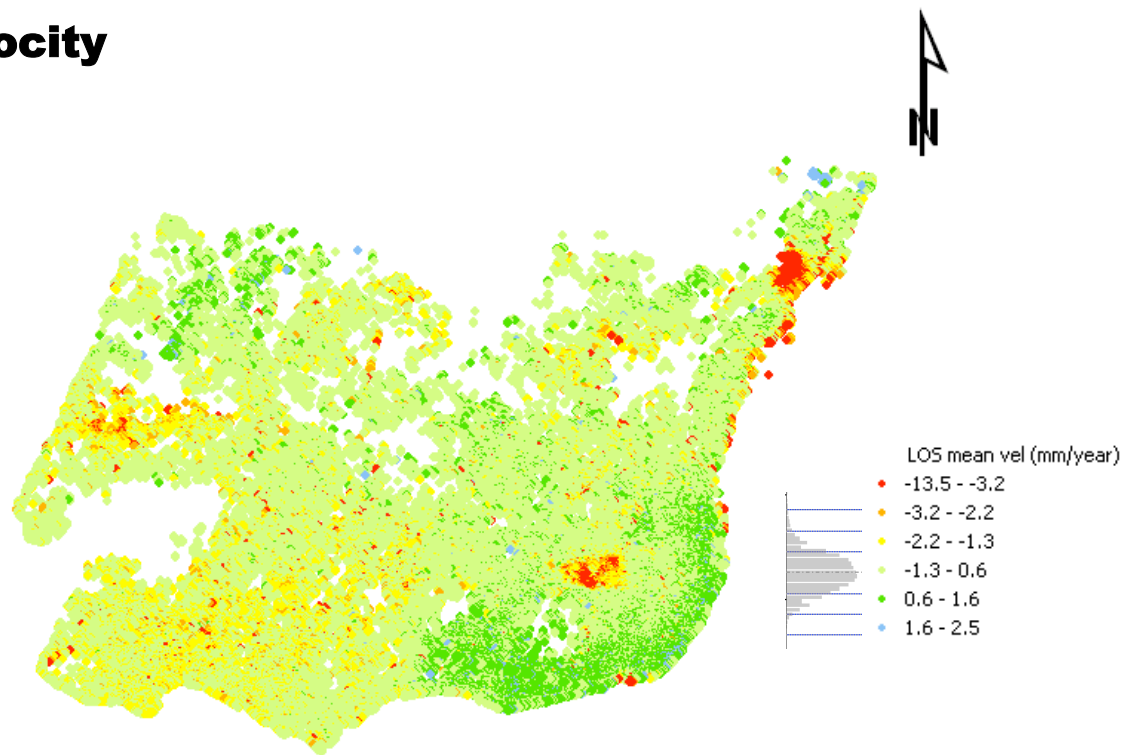
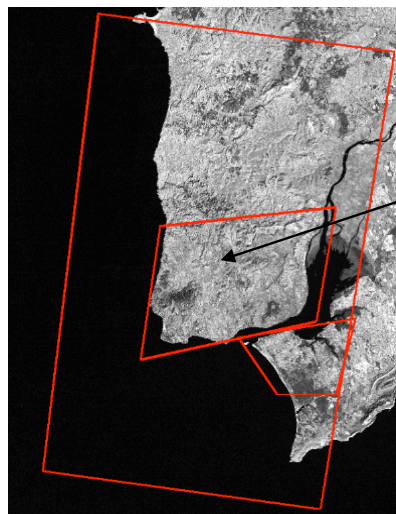
Date range of analysis: July 1992 to October 2006

Satellite data used: ERS -1/2 and Envisat

Georeference (X,Y) accuracy: 5 m

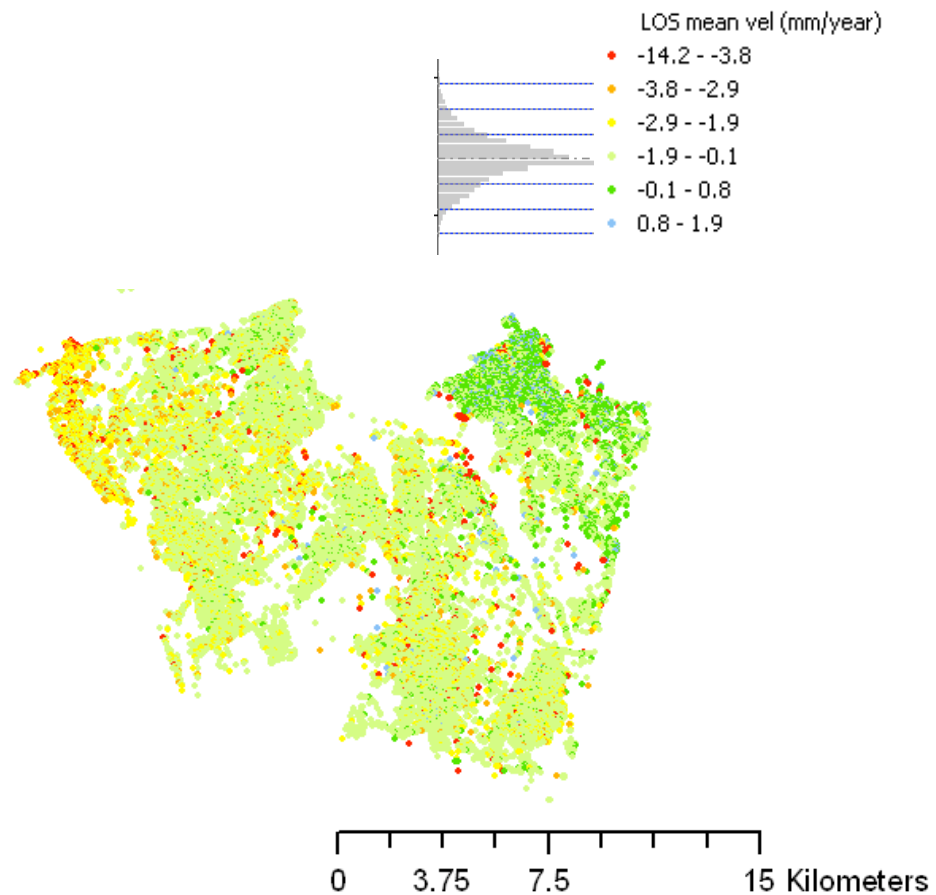
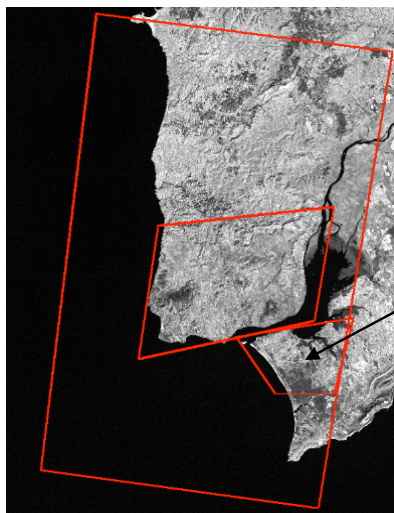
Reference point location: 486443.62 E 4279494.9N

Altamira North LOS Mean Velocity



Altamira South LOS Mean Velocity

Distinct reference
point



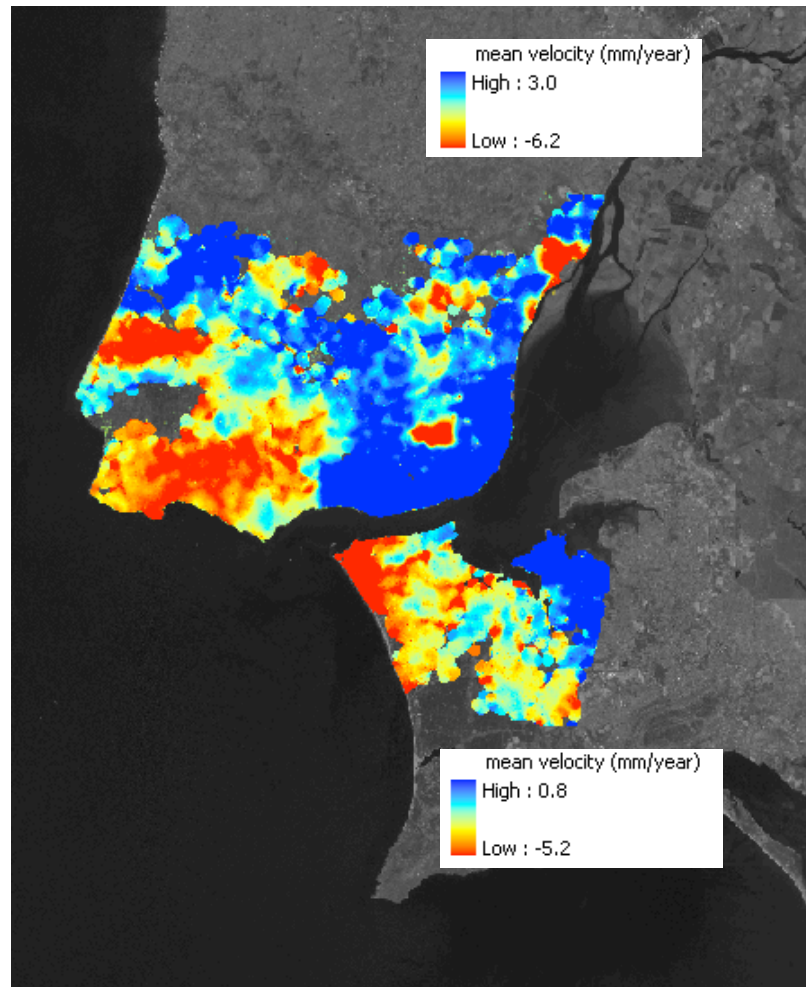
LOS Mean Velocity (mm/yr)

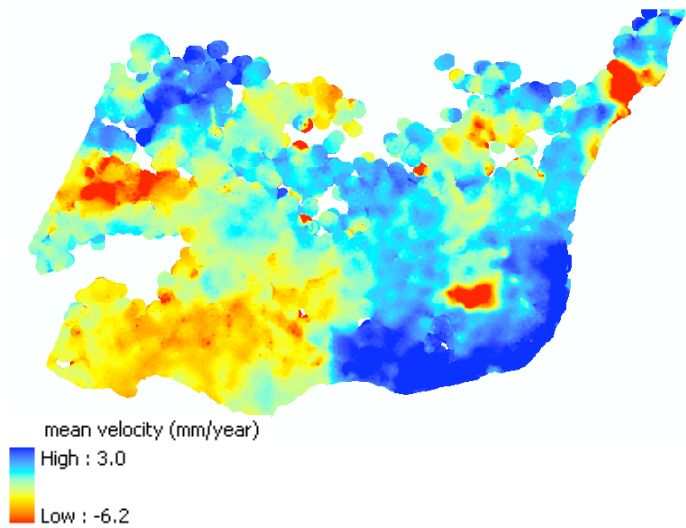
scatterer coherence > 0.5

IDW interpolation

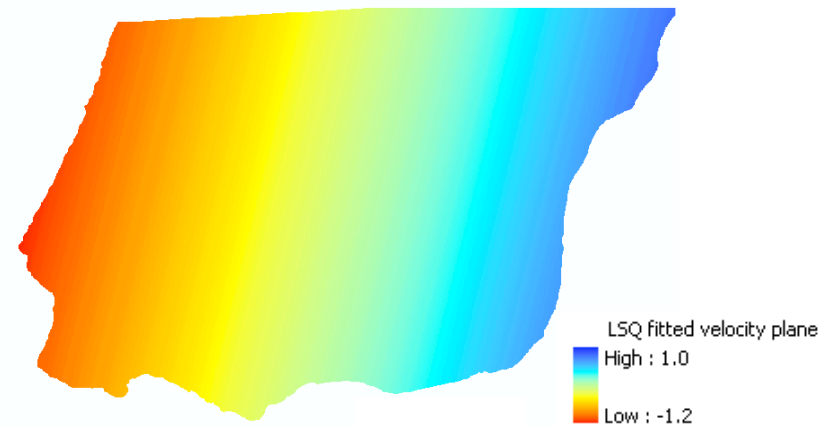
(cell=50m; radius=500m)

**North and South regions
have distinct reference
points**

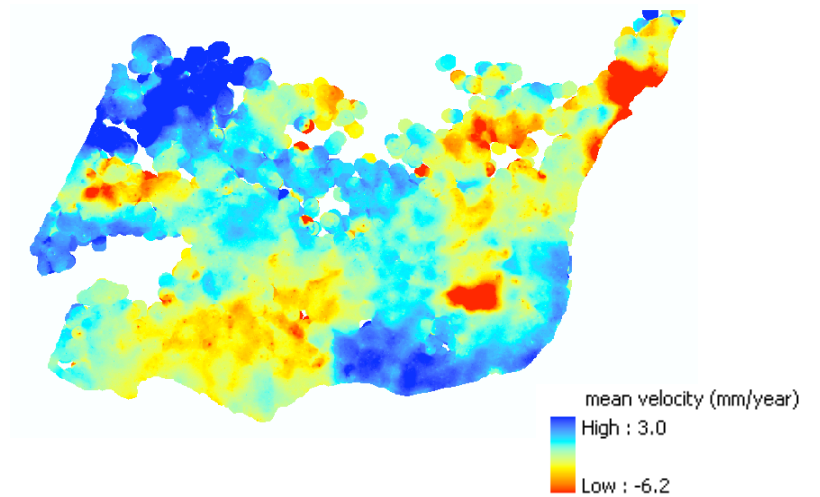




Maximum tilt direction \sim \perp to orbital track



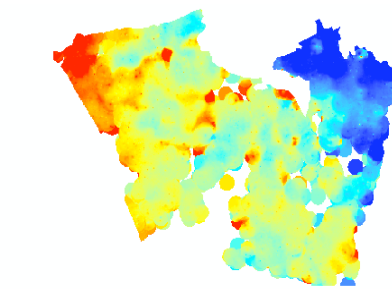
=



Altamira North:

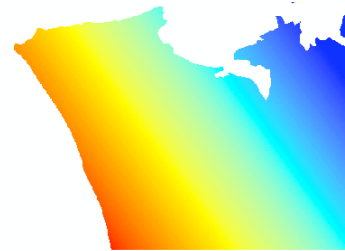
LSQ plane fitted and subtracted

Overall pattern is maintained



mean velocity (mm/year)
High : 0.8
Low : -5.2

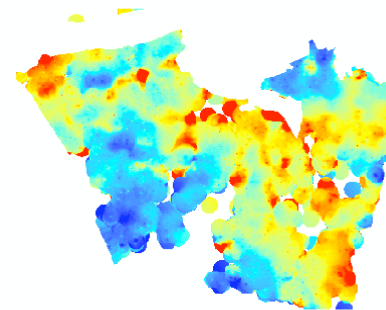
No orthogonality to satellite track



LSQ fitted velocity plane
High : 0.5
Low : -2.3

—

=



mean velocity (mm/year)
High : 0.999015
Low : -4.009856

Altamira South:

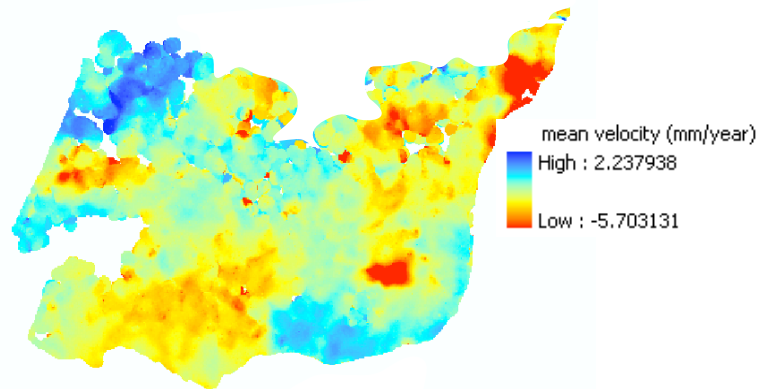
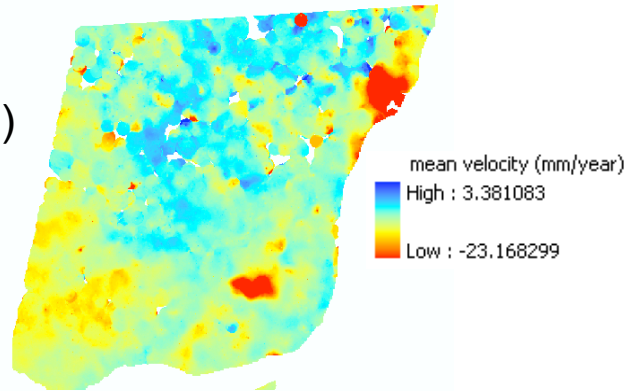
LSQ plane fitted and subtracted

Overall pattern is lost

LSQ plane is neither // nor \perp to orbital track

TRE detrended:

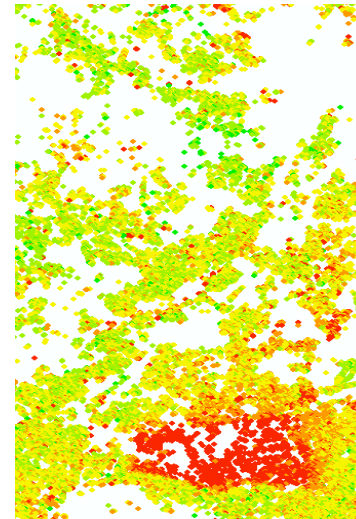
ERS1/2,
1992-2003,
55 scenes
(track 452 D)



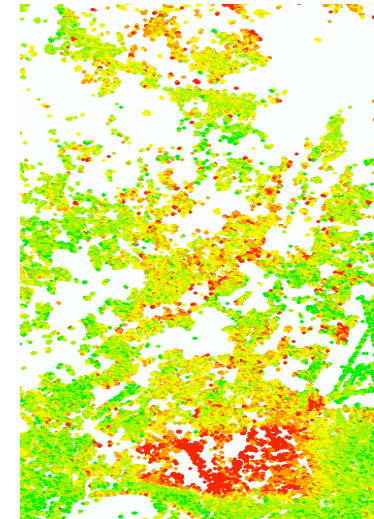
Altamira detrended: ERS1/2 & ENVISAT.
1992-2006, 100 scenes
(track 223 D)

Main difference:
Some NS lineaments absent
from TRE's map

TRE

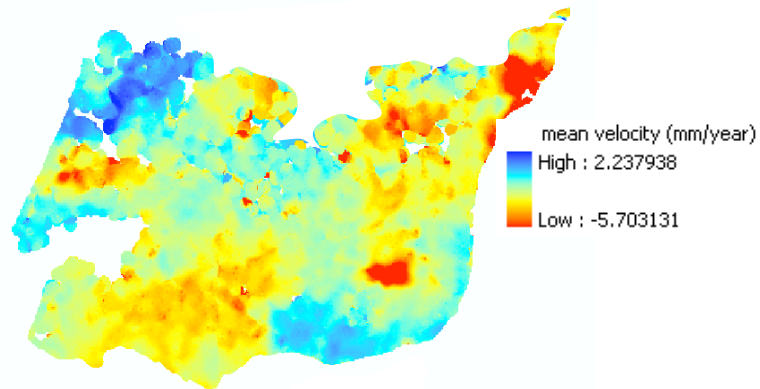
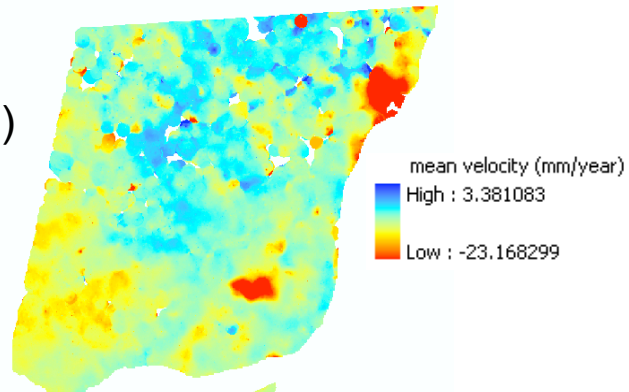


ALTAMIRA



TRE detrended:

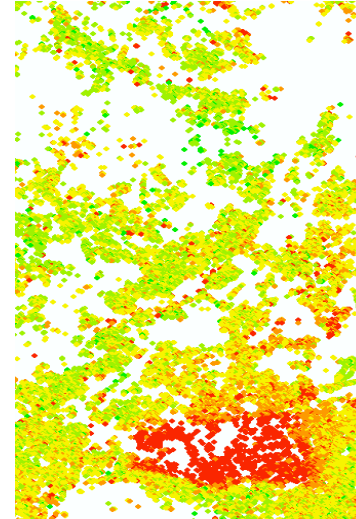
ERS1/2,
1992-2003,
55 scenes
(track 452 D)



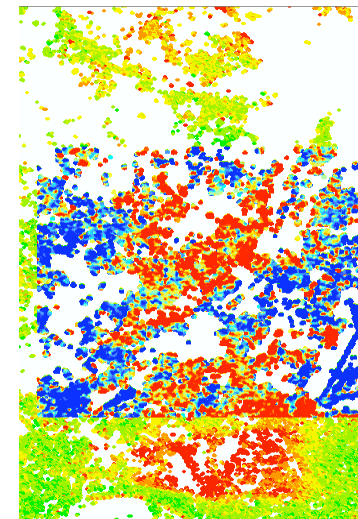
Altamira detrended: ERS1/2 & ENVISAT.
1992-2006, 100 scenes
(track 223 D)

Main difference:
Some NS lineaments absent
from TRE's map

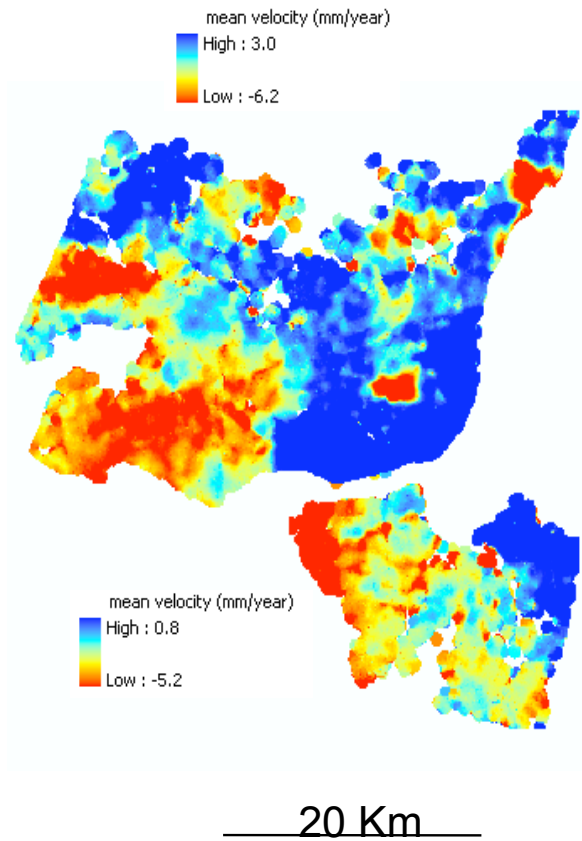
TRE



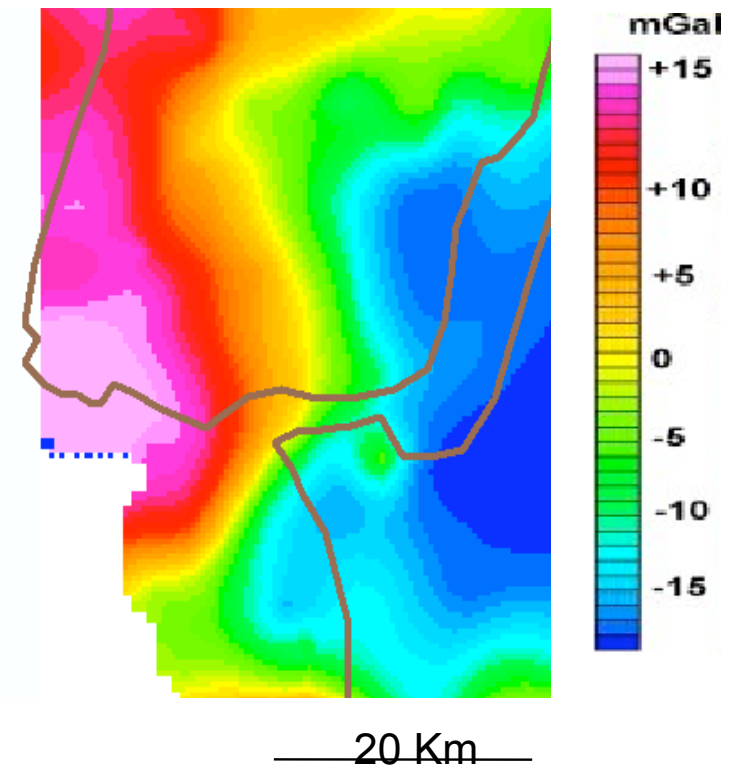
ALTAMIRA



Bouguer Anomalies (1st degree residuals)



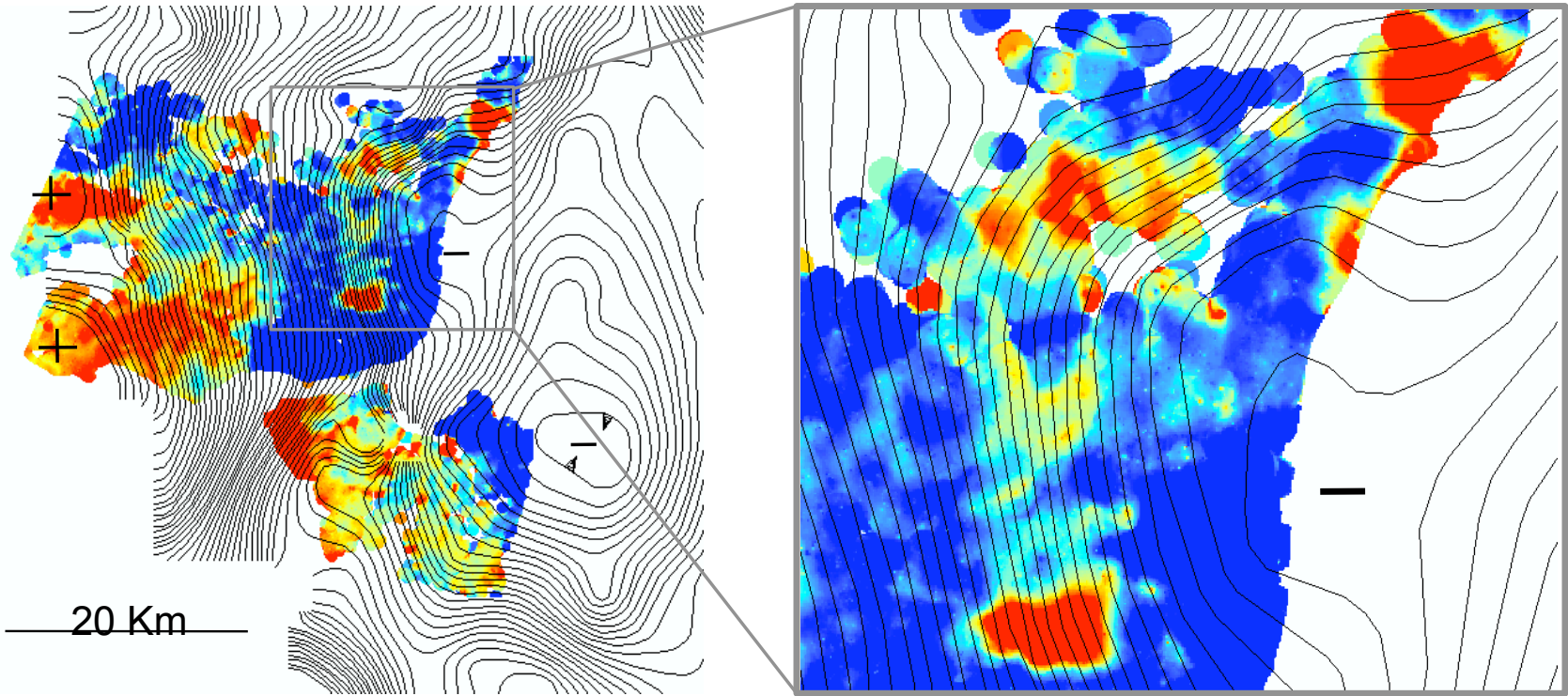
Torres, L., 2003



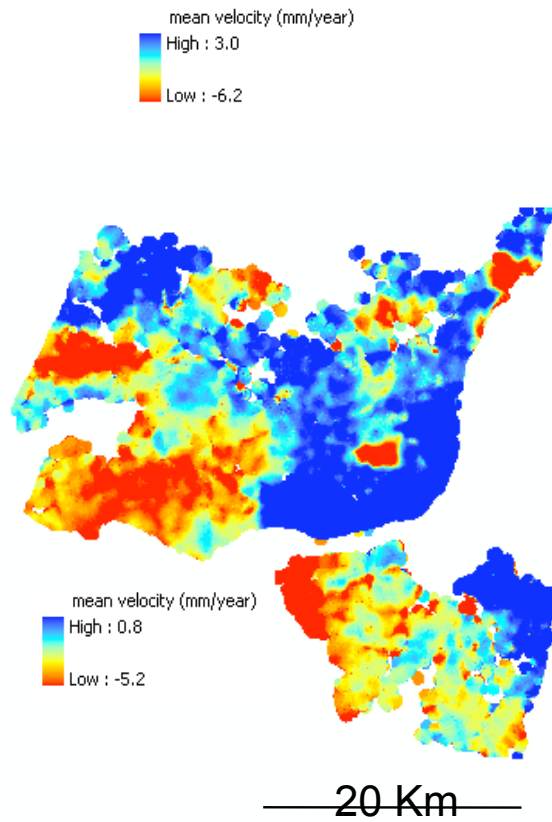
Bouguer Anomalies, 1st degree (isolines)

mean velocity (mm/year)
High : 3.0
Low : -6.2

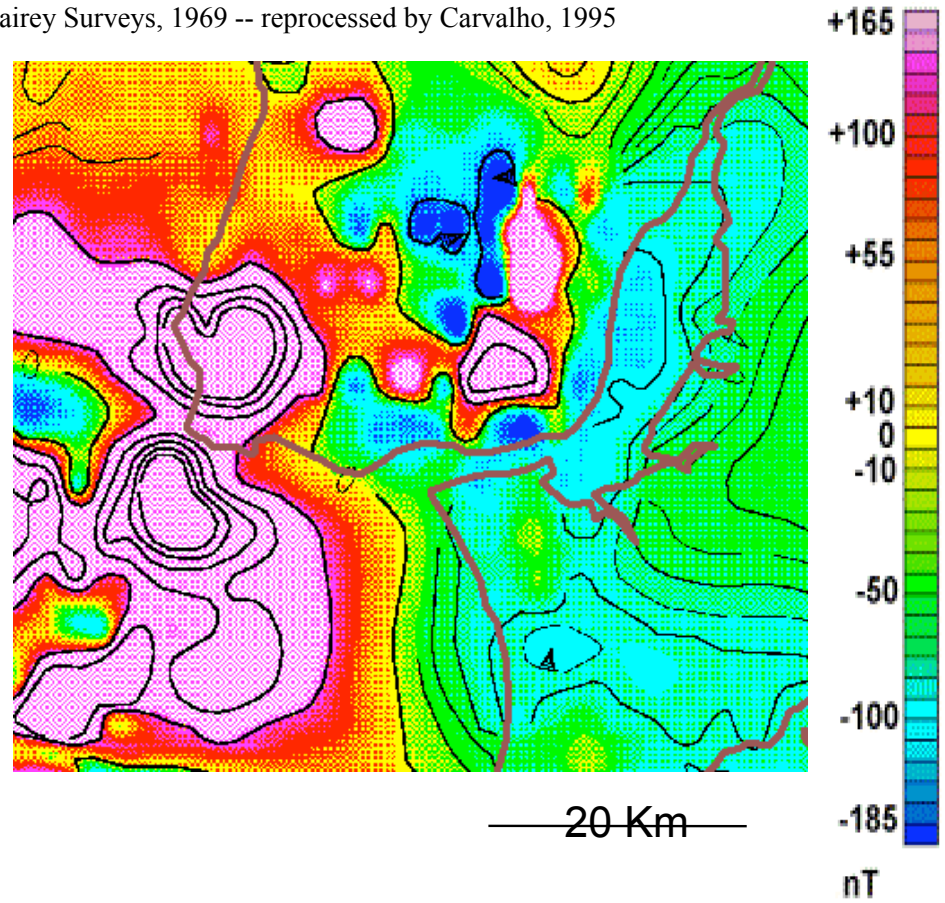
Torres, L., 2003



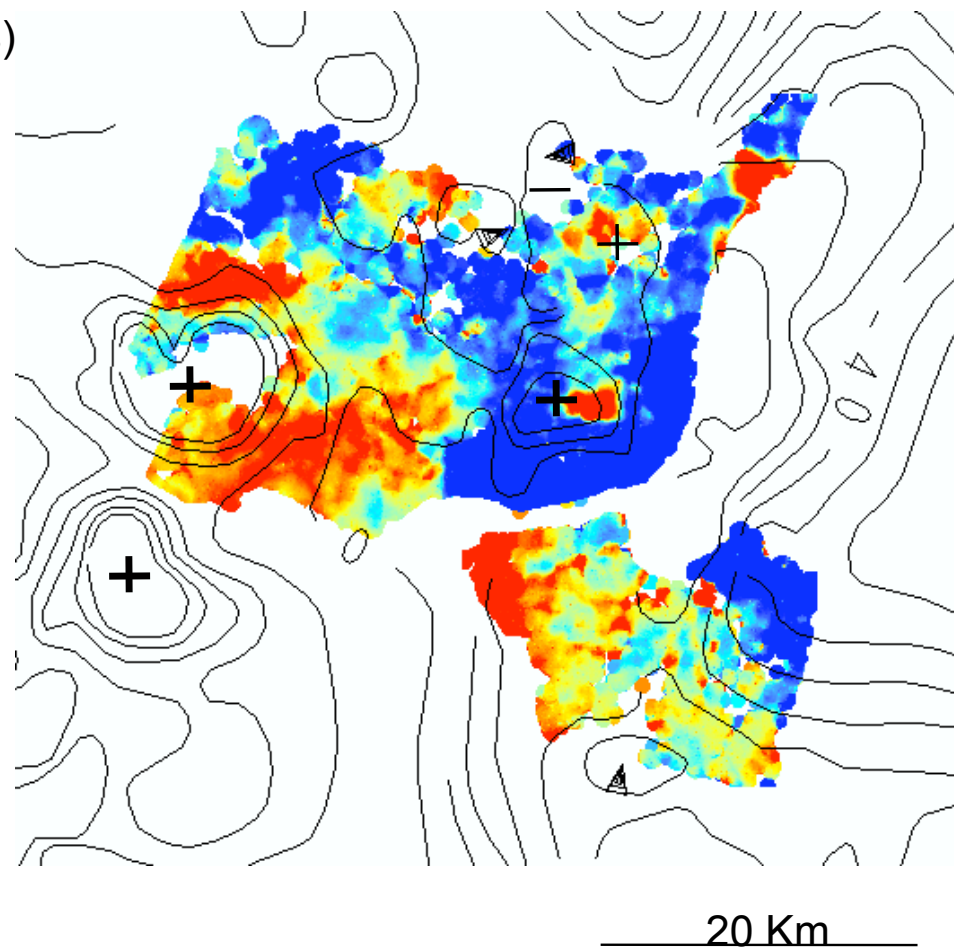
Aeromagnetic field



Fairey Surveys, 1969 -- reprocessed by Carvalho, 1995



Aeromagnetic field (isolines)



(Carvalho et al. EAGE, 2007)

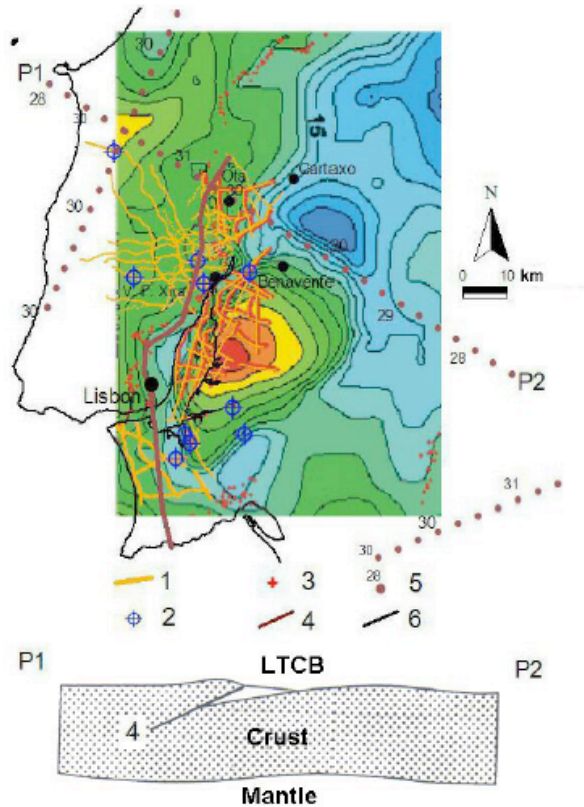


Fig. 3 Stripped gravity map of the study area (top) and (bottom) model of foreland basin after Cobbold et al. (1993). (1), (2) see legend of Fig. 1; (3) legend of Fig. 2; (4) proposed foreland basin fault zone; 5- Moho depths; 6-coastline.

(Carvalho et al. EMEEG, 2007)

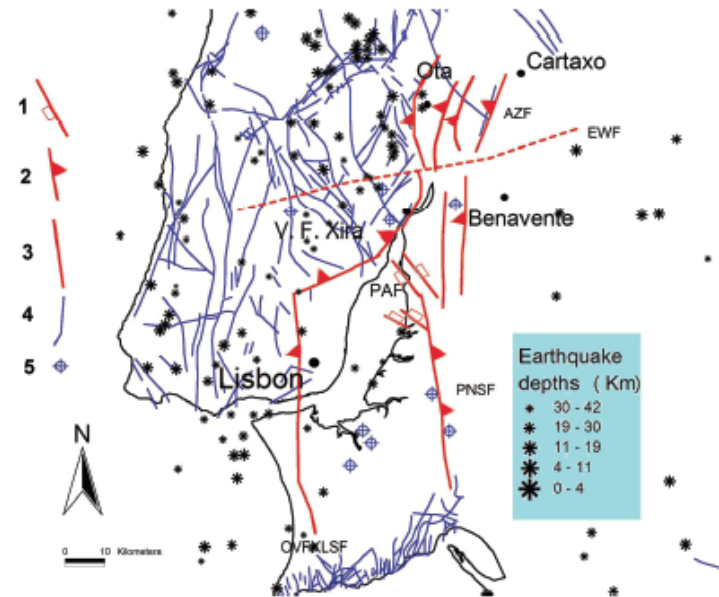
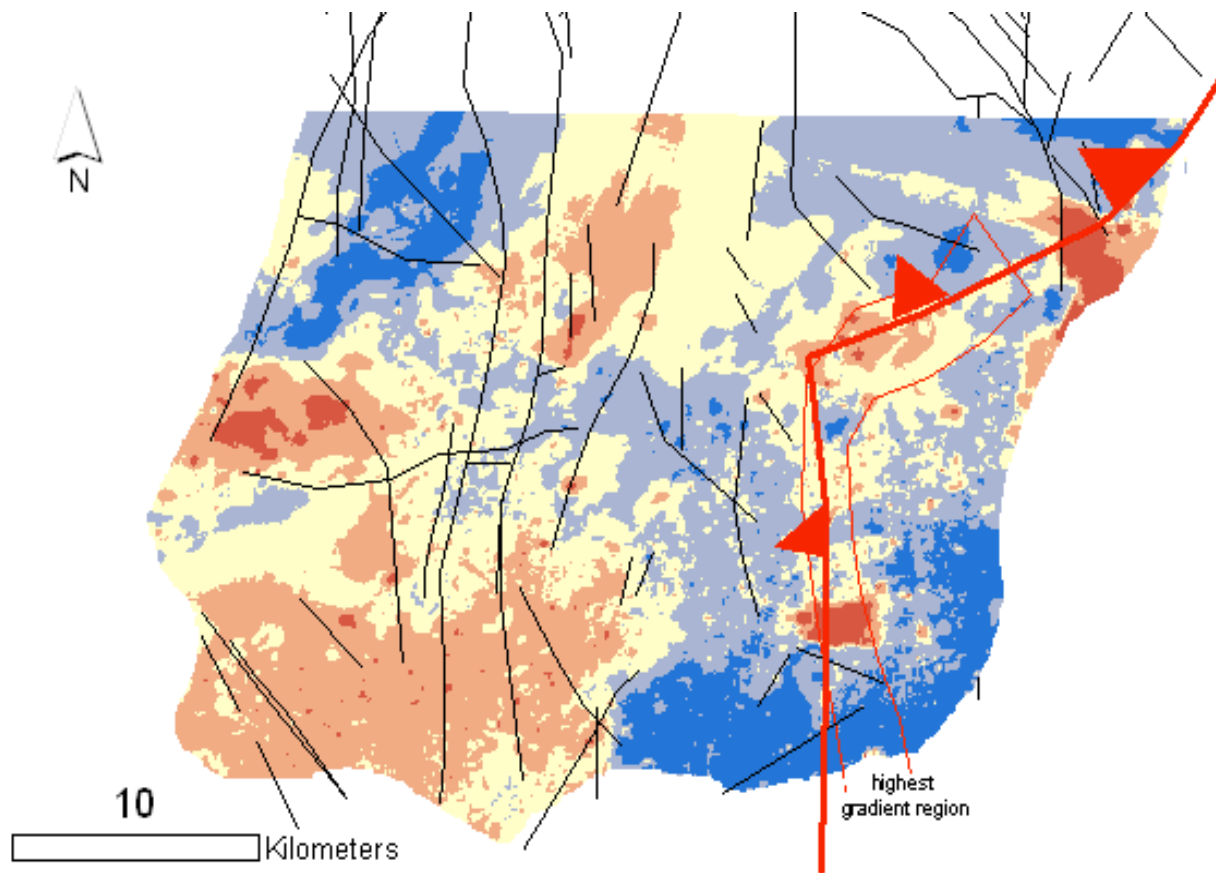
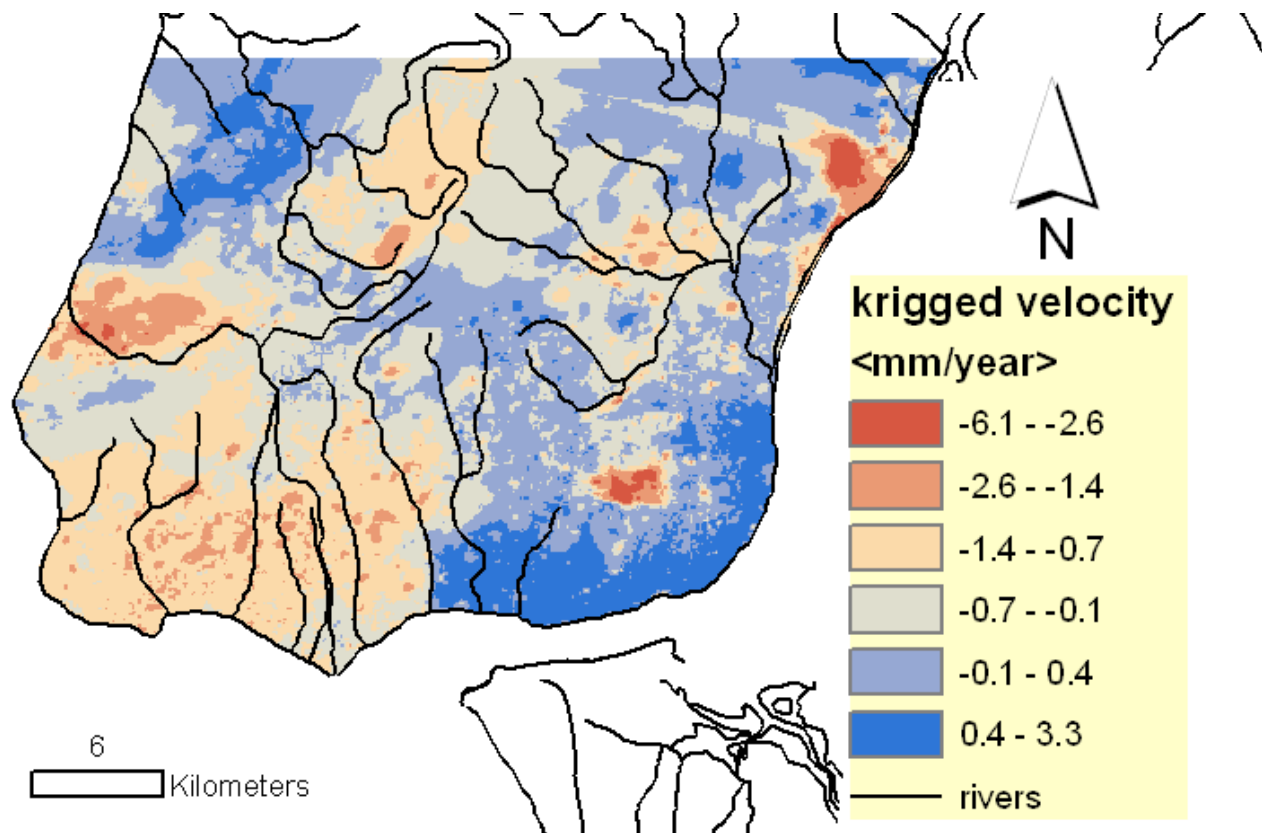
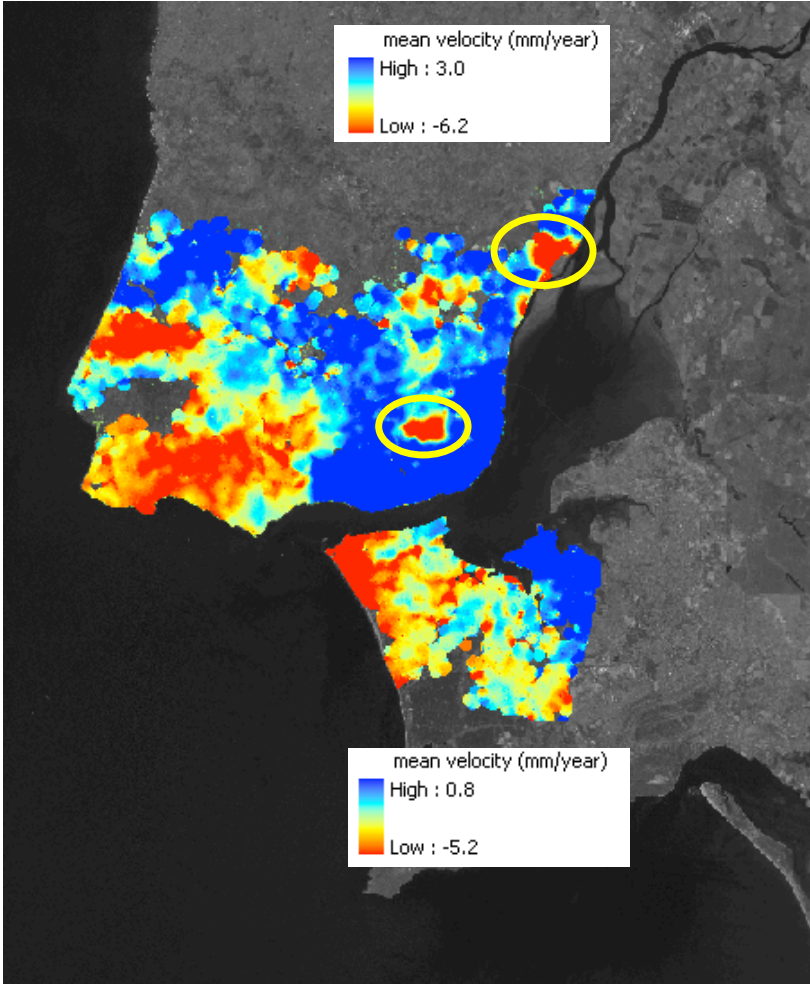


Fig. 3 – Final map with fault interpretation affecting an intra-Neogene horizon (approximate top of Upper Miocene). 1- normal fault (marks on lower block); 2- reverse fault (marks on upper block); 3- strike-slip or unknown movement fault. PNSF-Pinhal Novo-Setúbal fault; AZF- Azambuja fault; PAF- Porto Alto fault; OVFXLS- Ota-V.F. Xira-Lisbon-Sesimbra fault; EWF- E-W postulated fault (see text); 4- outcropping faults (after Oliveira et al., 1992); 5- wells.

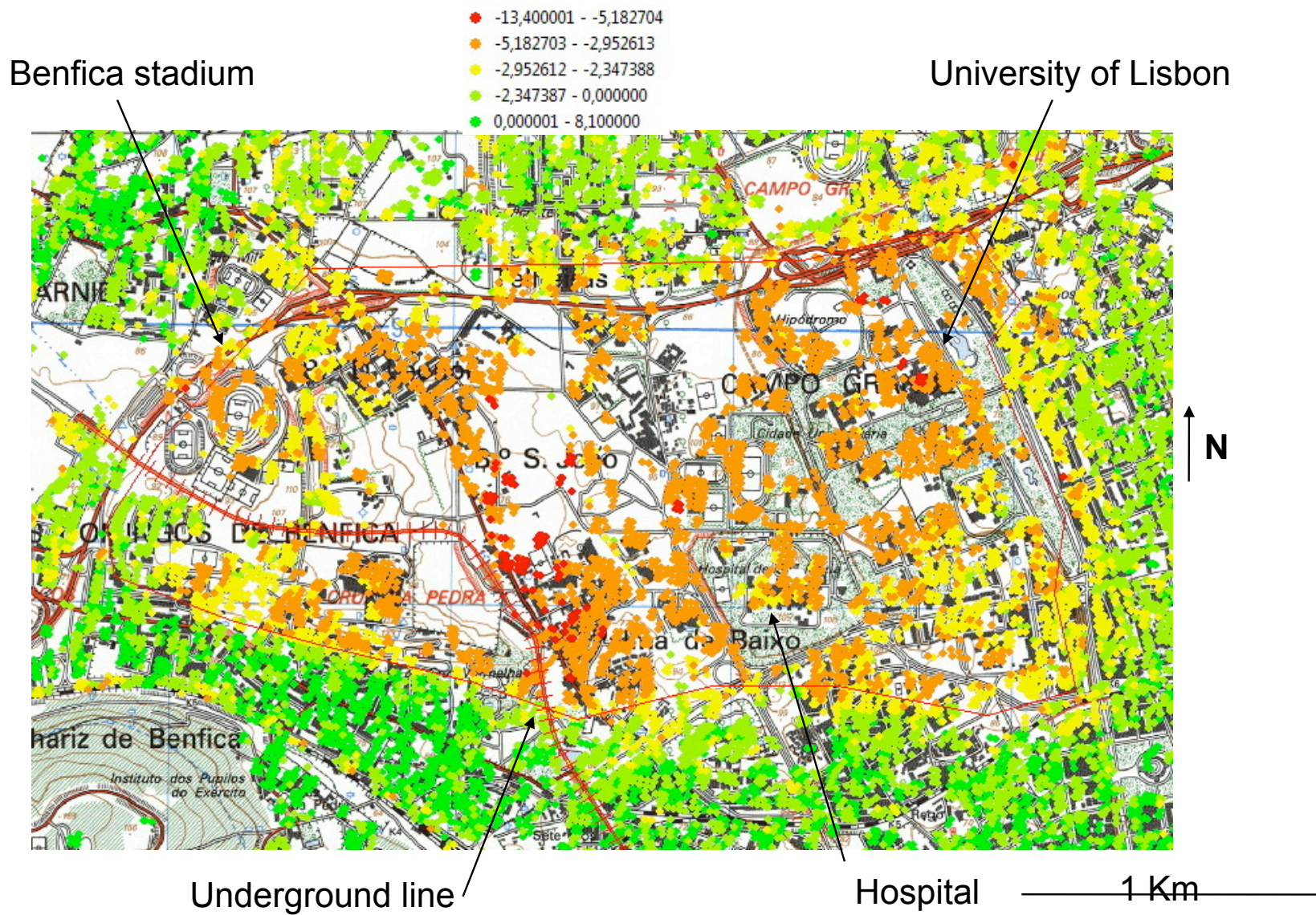




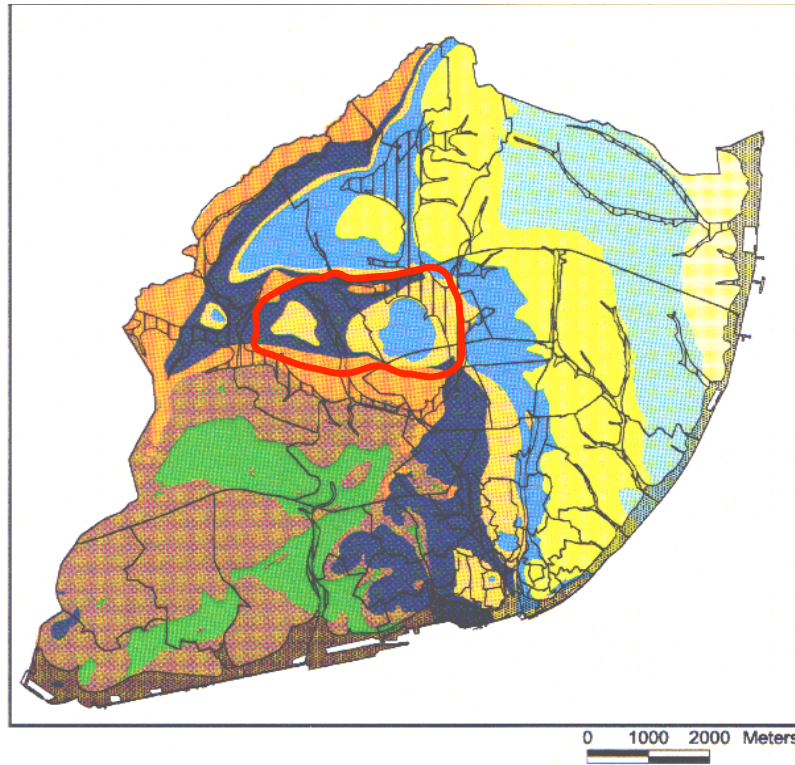
At a more local scale:



—20 Km—

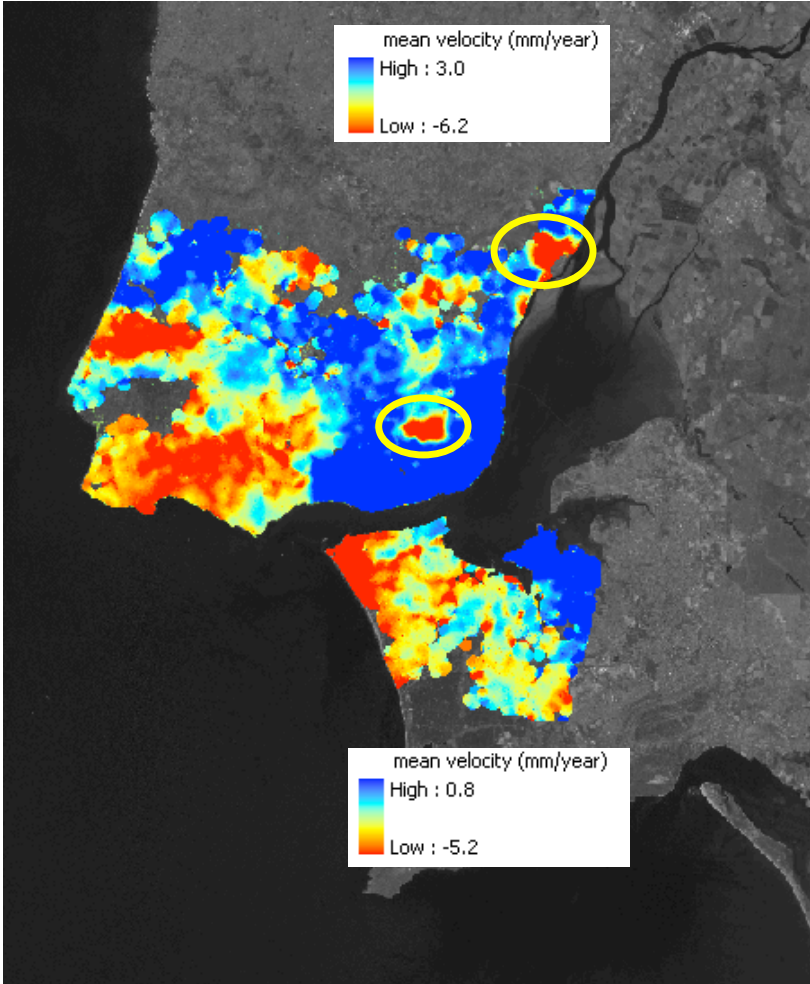


Lisbon simplified geological map, 1:10.000, CML

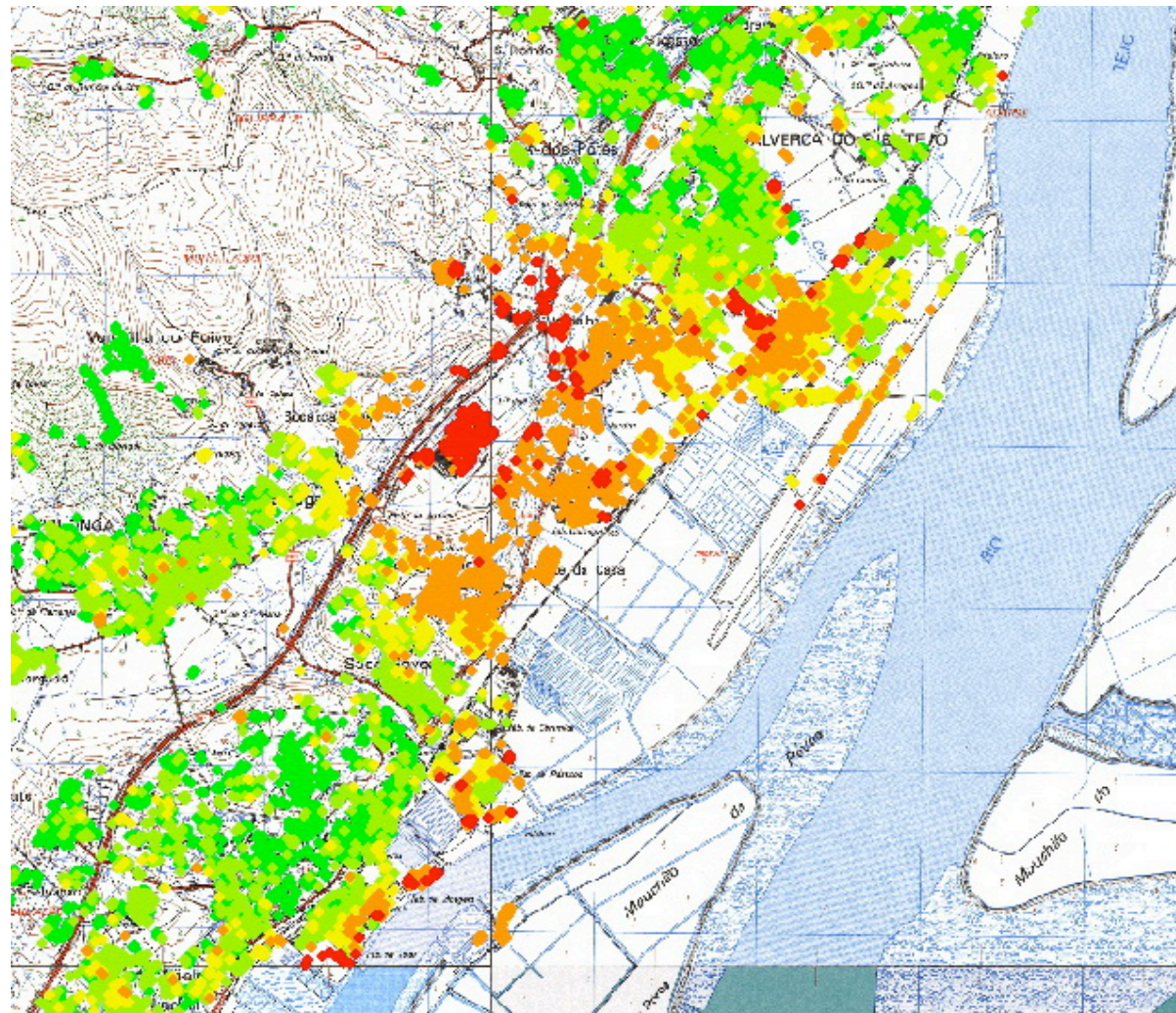


- Administrative borders
- Alluvium
- Tagus alluvium
- Upper Miocene sands and sandstones
- Upper Miocene clays and limestones
- Miocene sands and sandstones
- Miocene clays and limestones
- Lower Miocene sands and sandstones
- Lower Miocene clays and limestones
- Benfica Complex (Oligocene)
- Volcanic Complex (Up. Cretaceous)
- Limestones (Cretaceous)

At a more local scale:

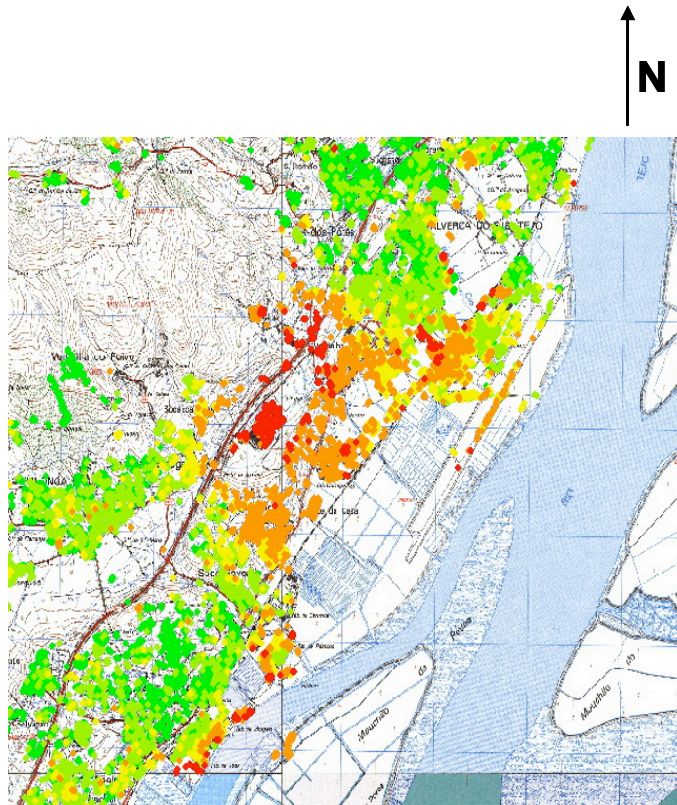


—20 Km—



- -13,400001 - -5,182704
- -5,182703 - -2,952613
- -2,952612 - -2,347388
- -2,347387 - 0,000000
- 0,000001 - 8,100000

3.5 Km



- -13,400001 - -5,182704
- -5,182703 - -2,952613
- -2,952612 - -2,347388
- -2,347387 - 0,000000
- 0,000001 - 8,100000

— 3.5 Km —



elevation
350m
0

— 3.5 Km —

Statement of Purpose -- January 2008 to December 2012

The line of research I intend to follow as senior researcher at ICIST will be centered on the use of SAR imagery to measure ground displacements with InSAR techniques (differential InSAR and PSINSAR).

I have selected the Lisbon region (Greater Lisbon and Setúbal Península) as my preferred study area.

I will focus my attention on two important problems in urban and suburban areas, namely:

- i) ground subsidence related to groundwater pumping
- ii) subsidence due to soil compaction, tunneling or other engineering works, and deteriorating structural foundations.

I also intend to investigate the potential of PSInSAR to monitor tectonic-driven crustal deformation, with a view to earthquake forecasting. This work builds on preliminary results obtained under the scope of project GMES TERRAFIRMA.

THANK YOU FOR YOUR ATTENTION

OBRIGADA PELA VOSSA ATENÇÃO